A Histological Analysis of the Hadrosaurid Dental Battery

by

Katherine Keenan Bramble

A thesis submitted in partial fulfillment of the requirements for the degree of

Master of Science

in

Systematics and Evolution

Department of Biological Sciences
University of Alberta

Abstract

The first histological study of an entire hadrosaurid dental battery provides a better understanding of this complex structure. The hadrosaurid dental battery is composed of interlocking, vertically stacked columns of teeth that form a complex grinding surface. The dental battery was previously considered to be a solid, cemented structure based on superficial examination of intact batteries and thin sections of isolated teeth. This first description of the dental battery using thin sections through the entire structure refutes the model of a single, fused mass of teeth. These thin sections confirm the presence of periodontal ligament connections between all teeth, underscoring its dynamic nature. The serial thin sections across an adult dental battery also revealed signs of gradual and possibly ontogenetic tooth migration. These signs include the extensive remodeling of the alveolar septa and the anteroposterior displacement of successive generations of teeth. The four most posterior tooth families migrated posteriorly whereas the remaining tooth families had a progressively more pronounced anterior trajectory. This migration is pronounced enough in some areas to cause extensive resorption of neighbouring teeth. Thin sections through a dental battery of a perinatal specimen reveal that all of the alveolar septa are angled anteriorly, which suggests that extensive and unidirectional tooth migration begins early in ontogeny and that any additional migration happens later in ontogeny. Although the mechanisms behind tooth migration in the hadrosaurid dental battery require further investigation, addition of tooth families during growth and opposition of forces during palinal mastication may have had a strong influence.

Focusing on the individual hadrosaurid teeth shows that they exhibit a highly specialized arrangement of hard tissues to allow each tooth to be ground down completely.

Histological thin sections of teeth from the hadrosaurid dentary and the mammalian ever-growing incisor reveal surprising similarities in morphology and hard tissue organization. These similarities include the shift of the cemento-enamel junction to form a cutting edge along the occlusal surface. Similar to modern rodents and lagomorphs, the wear of the softer dentine and cementum, continuous eruption, and plugging the pulp cavity allowed hadrosaurid teeth to form a continuously replenished wear surface. The mammalian ever-growing incisor thus serves as an unexpectedly accurate model for dentinogenesis in the hadrosaurid tooth. The mammalian ever-growing incisor is a valuable extant analogue for understanding the perceived complexity of the hadrosaurid tooth than previously proposed models. Using this model, a heterochronic shift in dental ontogeny was inferred between neonatal and adult hadrosaurids as dentinogenesis is inferred to function at a different rate in the adult hadrosaurid. A new subtype of primary dentine, crestal dentine, was also revealed during this study. Crestal dentine has an increased hardness based on its chemical composition and tubular structure, which allows it to functionally replace the enamel that is lost in older functional tooth generations of a tooth family.

Preface

Chapter 2 of this thesis has been submitted for publication as K. Bramble, A. R. H. LeBlanc, D. O. Lamoureux, M. Wosik, and P. J. Currie, "Histological evidence for a dynamic dental battery in hadrosaurid dinosaurs with evidence of tooth migration," to Scientific Reports, on July 12, 2017. K.B wrote the manuscript, K.B and M.W made the histological sections, K.B, A.R.H.L, and D.O.L. interpreted the data, P.J.C supervised the work, and all authors contributed to editing the manuscript.

Selected Quotes

"The microscopical examination of the structure of the Iguanodon's teeth thus contributes additional evidence of the perfection of their adaptation . . . [T]heir truth and beauty become more manifest as our knowledge of their subject becomes more particular and exact."
- Owen 1840, p. 252, [Iguanodon is a type of hadrosaurid]

~~~~~~~~~~~~~~~

"The teeth in the hadrosaurian dinosaurs have reached the highest degree of perfection and numbers in any known reptile"
- Lull and Wright 1942, p. 67-68

~~~~~~~~~~~~~~~

"Dinosaurs Rule!"
- Katherine Bramble (personal quote since elementary school)

Acknowledgements

First, I would like to thank my supervisor, Philip Currie for his guidance throughout my program and allowing me to change up my project so late in the game. Thanks also to Eva Koppelhus for her help throughout the years. I would also like to thank Rob Holmes, my committee member, who, along with John Acorn and Sydney Mohr, formed my "subcommittee". They helped make sure both my thesis and me were heading in the right direction.

I would like to thank the following people for providing access and assistance during my museum collections visits: C. Mehling (AMNH), J. Mallon, K. Shepard, and M. Currie (CMN), J. Horner and J. Scannella (MOR), D. Evans, K. Seymour, and B. Iwama (ROM), B. Strilisky and R. Sanchez (RTMP). From the University of Alberta, I thank B. Barr (UAMZ) for the modern specimens I sliced and diced, H. Gibbins (UALVP) for his help with specimens and inquiries, and C. Coy (UALVP) for putting up with my many questions over the years.

As well, I thank D. Evans for use of the Royal Ontario Museum Palaeohistology Lab, microscope, and imaging software. Thanks to G. Funston, M. Wosik, and A. LeBlanc for showing me the ropes in the histology lab. M. Caldwell provided access to his extant histological slide collection, and both he and E. Koppelhus provided access to microscopes and imaging software as well. All of which have been used heavily in creating this thesis. Also, thank you to the University of Alberta Advanced Microscopy Facility for the use of their pika thin sections.

I thank my Currie Lab cohort, V. Arbour, G. Bradley, M. Burns, G. Funston, B. Kruk, S. Mohr, WS. Persons IV, M. Rhodes, B. Stettner, and A. Torices for their help with this and

other projects. To them, and the non-dinosaur paleontology graduate students, who were my office mates, thank you for the discussions, writing assistance, office shenanigans, friendship, and many cups of tea. This includes M. Campbell-Mekarski, P. Jiménez Huidobro, I. Paparella, T. Simões, S. Sinha, H. Street, O. Vernygora. I also thank A. Lindoe for giving me a run for my money in the pun department. M. Biesterfeldt and C. Gilmore also provided food, laughs, and cheerleading when needed.

I am indebted to A. LeBlanc for infecting me with the dental histology bug and helping me through the confusion, excitement, and many, many questions. I also thank him for the use of two of his histological images for this thesis. I also greatly thank D. Lamoureux for endless discussions and clarifications about the world of dental histology. M. Wosik was also an amazing help with this thesis as he taught me how to make the dental battery histological thin sections and continued to work on the unfinished slides after I had to leave the ROM Palaeohistology Lab and head back to Edmonton.

I am very grateful for the funding and scholarships I received from the National Sciences and Engineering Research Council, the Alberta Lottery Fund, the Alberta Historical Resources Foundation, The University of Alberta Faculty of Graduate Studies and Research, the Graduate Student Association, the Faculty of Science, and the Department of Biological Sciences.

Finally, I would like to thank my family. Mom, words cannot express the amount of gratitude I have for all you have done. I would also like to thank my siblings, Michael and Jerrilyn, for always being there for me, and thank you Bunny for the soft encouragement. Hooman, I could not have done this without your laughs, support, and cooking skills. Dad, I wish you could have been here to see this.

Table of Contents

List of Figures

Chapter 1

Chapter 2

Chapter 3

List of Abbreviations

Institutional Abbreviations

ROM, Royal Ontario Museum, Toronto, Canada

UALVP, University of Alberta Laboratory for Vertebrate Paleontology, Edmonton, Canada

Anatomical Abbreviations

CDJ, cemento-dentine junction

CEJ, cemento-enamel junction

DEJ, dentine-enamel junction

The reader is referred to the figure captions for the anatomical abbreviations that are specific to each figure.

Chapter 1: Introduction

1.1. General overview

Hadrosaurids are a clade of large extinct unarmoured herbivorous dinosaurs that were dominant in their ecosystems. Commonly referred to as ‘duckbills’ for their broad, flat edentulous keratinized cropping bills, they, along with ceratopsids (horned dinosaurs) and ankylosaurs (arnoured dinosaurs) comprised the dominant herbivorous megafauna of the Late Cretaceous terrestrial ecosystems of North America. The two subfamilies of hadrosaurids are Hadrosaurinae and Lambeosaurinae (Figure 1.1), following the traditional taxonomy for the Hadrosauridae (Horner et al. 2004, Xing et al. 2014). Hadrosaurine hadrosaurs are usually crestless, but can also have a crest of solid bone (Brett-Surman 1979, Horner et al. 2004), or a crest made of soft tissue (Bell et al. 2014) (Figure 1.1a). Lambeosaurine hadrosaurs, on the other hand, have hollow supranarial crests (Brett-Surman 1979, Horner et al. 2004) that developed into bizarre shapes in some species (Brown 1914, Parks 1922, Evans and Reisz 2007) (Figure 1.1b).

Many aspects of hadrosaur anatomy, biology, ecology, distribution, and relationships have been studied, including growth dynamics (Vanderven et al. 2014, Woodward et al. 2015), evolution and function of their characteristic skulls (Ostrom 1961, Dodson 1975, Smith and Dodson 2003, Evans 2010, Brink et al. 2014), herding behaviour and biogeography (Brett-Surman 1979, Fiorillo and Gangloff 2001, Prieto-Márquez 2008, Fricke et al. 2009), paleoecology (Fastovsky and Smith 2004, Gates 2007, Gangloff and Fiorillo 2010), as well as cranial and postcranial phylogenetic characters (Brett-Surman and Wagner 2007, Prieto-Márquez 2008).

Figure 1. 1. Representatives of Hadrosauridae. **a**, *Edmontosaurus regalis*, a hadrosaurine; **b**, *Parasaurolophus walkeri*, a lambeosaurine. Images not to scale. Images copyright Scott Hartman, used with permission.

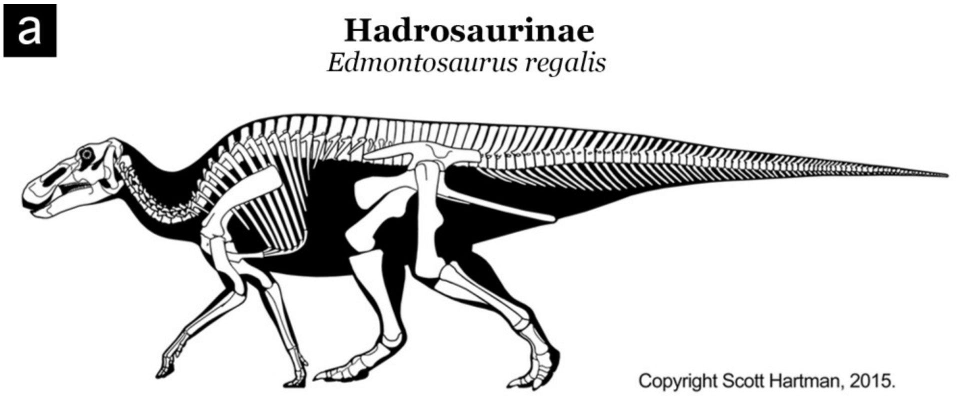
a
Hadrosaurinae
Edmontosaurus regalis
Copyright Scott Hartman, 2015.

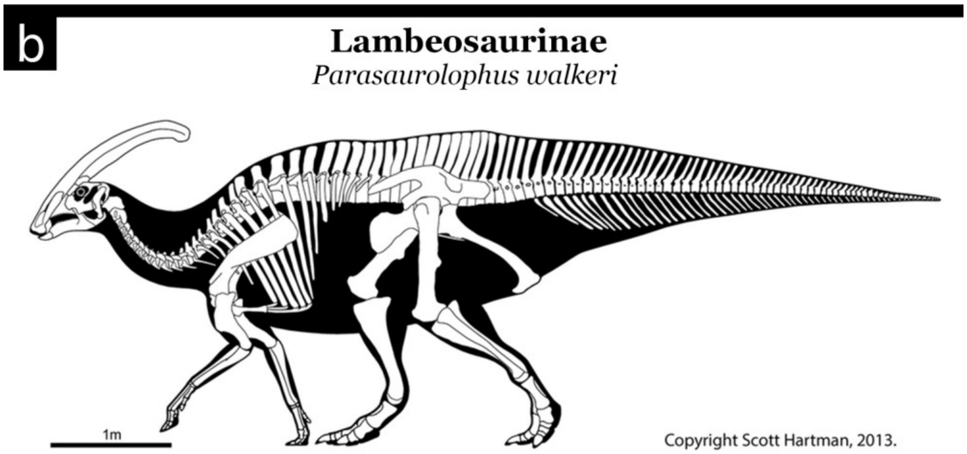
b
Lambeosaurinae
Parasaurolophus walkeri
1m
Copyright Scott Hartman, 2013.

One of the most striking features of hadrosaurids is their specialized dental apparatus, called a dental battery, which is unlike anything seen in modern herbivores. However, dental studies have only concentrated on tooth replacement (Edmund 1960), tooth wear (Williams et al. 2009, Mallon and Anderson 2014), and jaw biomechanics (Weishampel 1983, Nabavizadeh 2014, Mallon and Anderson 2015). Not as much work has been conducted on the internal structures of the dental battery, with only recent exceptions (Erickson et al. 2012, Erickson and Zelenitsky 2014, Wang et al. 2015, Brink et al. 2016, LeBlanc et al. 2016b). These studies have focused on individual teeth or the dental battery in coronal cross section, and have opened up new opportunities and questions for investigation. Ontogenetic variation within the dental battery is difficult to ascertain as the teeth formed an uninterrupted structure of interlocking teeth (Cope 1883, Ostrom 1961, Erickson et al. 2012, Erickson and Zelenitsky 2014), making it difficult to study individual teeth or their mutual spatial relationships in any detail. To properly study this unique structure, an internal histologic view of the entire dental battery is necessary.

1.2. The hadrosaurid dental battery

Hadrosaurs are one of the most abundant and diverse groups of dinosaurs, with skeletons known for all age categories, including embryos (Horner et al. 2004). They were grazing animals with a diet that consisted of hornworts, liverworts, lycopsids, ferns, horsetails, fruit, as well as the twigs, bark, and seeds of angiosperms and conifers (Chin 2007, Tweet et al. 2008, Williams et al. 2009, Erickson et al. 2012, Mallon and Anderson 2014). This plant material, and possibly soil picked up from grazing low vegetation, contributed to the wear of their teeth (Williams et al. 2009). To effectively process such a diet, as well as compensate for the amount of tooth wear that inevitably resulted, hadrosaurs evolved a specialized dental complex called the dental battery.

The dentary (Figure 1.2), the largest bone of the lower jaw, forms two-thirds the length of the mandible and bears the lower dental battery. Its short anterior edentulous portion articulates with the predentary, which bears the lower half of a keratinous bill, or rhamphotheca (Morris 1970, Nabavizadeh 2014). Laterally, the dentary contacts postdentary bones, including the articular, which forms the lower half of the jaw joint. The large coronoid process extends dorsally from the posterior region of the lateral side of the dentary and does not participate in the margin of the tooth row. Laterally, the elongate dentary has a smooth surface bearing multiple foramina. The medial surface supports the dental battery, which is formed by multiple vertical tooth families, each with nutrient foramen at its base. The series of alveoli for this battery is the most prominent feature of the dentary.

The anatomy of the hadrosaur dental battery is highly specialized and unlike anything seen in extant species. The lanceolate teeth (Figure 1.2b) have lingual facing crowns, which in life would have been covered basally by a thin boney wall called a lingual plate (Lull and Wright 1942). Each enamel covered tooth crown has a median carina and most species have marginal denticles. Some workers consider hadrosaurid teeth have reached the highest level of perfection (Lull and Wright 1942). The teeth interlock with those of the adjacent tooth rows, forming a robust, continuous dental pavement or battery. The dental battery tapers dorsoventrally at the anterior and posterior ends as the teeth become smaller. A single dental battery can have up to 60 tightly packed tooth columns, or tooth families, with each having three to six successional teeth (Lull and Wright 1942, Ostrom 1961). These teeth were suspended in place within the jaw and to adjacent teeth by periodontal ligaments (LeBlanc et al. 2016b). The occlusal surface (Figure 1.2c) comprises two to four teeth from each tooth family, and has the appearance of tessellated pavement. A coronal view of a tooth family shows the axis of each tooth to be obliquely inclined (Figure 1.2e), which is how more than one tooth per family can be functional, with one tooth (the

Figure 1. 2. The hadrosaurid dental battery and dentition. **a**, UALVP 11734, right dentary, lingual view, anterior is to the left; **b**, UALVP 55127, an isolated hadrosaurid dentary tooth, lingual (left) and coronal (right) views; **c**, occlusal view of a hadrosaurid left maxilla (UALVP 99), white arrows indicating the presence of enamel, anterior is to the left; **d**, occlusal view of a hadrosaurid right dentary (CMN 351), white arrows indicating the presence of enamel, anterior is to the right; **e**, coronal view of the maxilla and dentary with each showing a cross section of a single tooth family, grey represents jaw bone, white represents teeth, black represents enamel. Abbreviations: ce, cementum; cej, cemento-enamel junction; db, dental battery; en, enamel; nf, nutrient foramen; tf, tooth family.

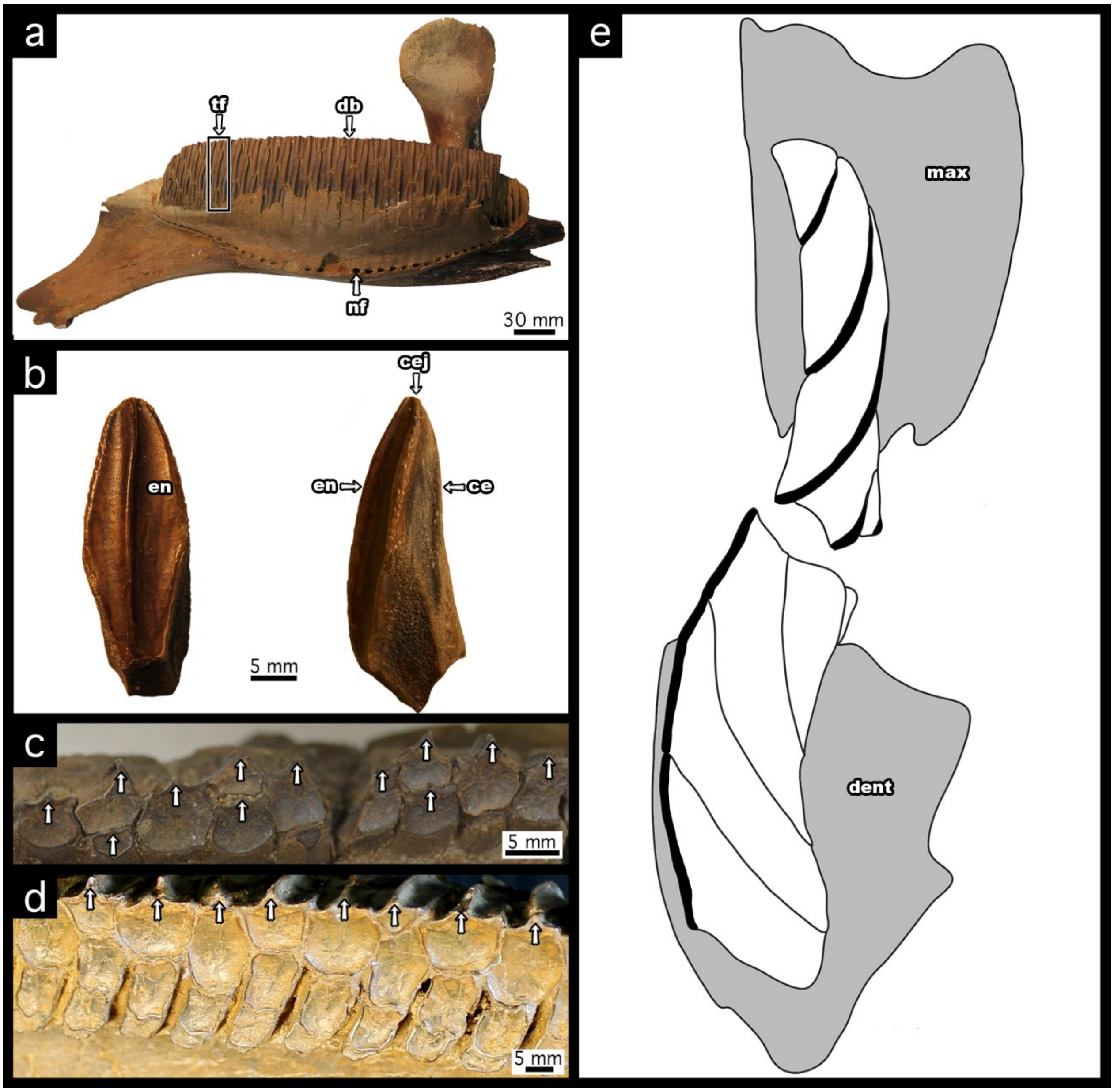
a
tf
db
nf
30 mm
b
en
cej
en
ce
5 mm
c
5 mm
d
5 mm
e
max
dent

oldest) largely worn away and ready to be shed, the next oldest forming the majority of the grinding surface, and often one or even two successively younger teeth moving into position and beginning to develop wear facets. These teeth are ground away and continuously replaced throughout life by the successive teeth of the next generations (Horner et al. 2004).

The anatomy of the maxillary dental battery is slightly different than that of the dentary. The enamel covers the labial face of the maxillary tooth crown, and as a result, more than one functional tooth per tooth family bears enamel (Horner et al. 2004) (Figure 1.2c, e). The teeth of the maxillary dental battery are slightly more narrow than those in the dentary, increasing the number of tooth positions in the maxilla (Horner et al. 2004). Wear surfaces on the maxillary and dentary occlusal surfaces give insight to how they occluded during mastication (Weishampel 1983, Mallon and Anderson 2014, Nabavizadeh 2014).

The closest comparison to the hadrosaur dental battery is that of ceratopsian dinosaurs, a contemporaneous megaherbivore. As in hadrosaurs, the ceratopsian dental battery (Figure 1.3a) consists of multiple rows of tightly packed, continuously replaced teeth; however, there are important differences. Ceratopsian tooth crowns are highly angled to their roots and are relatively broad in comparison with hadrosaur teeth (Figure 1.3b). This makes the dental battery less compact with approximately 15 fewer tooth rows per battery (Mallon and Anderson 2014). Ceratopsian dental batteries also generally have fewer successional teeth than hadrosaurs, having a maximum of five successional teeth depending on species and size (Dodson et al. 2004). Only one tooth per tooth family contributes to the occlusal surface, with the tooth family being more obliquely inclined than in hadrosaurids (Figure 1.3c). The ceratopsian dental battery specialized solely on shearing, unlike the hadrosaur battery, which also had a crushing and grinding function (Mallon and Anderson 2014). Hadrosaurs had a more generalized diet, while ceratopsians would have only eaten tough plant matter, leading to the idea that a similar diet may not have been the

Figure 1. 3. The ceratopsian dental battery. **a**, UALVP 41, ceratopsian dentary, lateral and medial view; **b**, UALVP 52997, isolated ceratopsian tooth in coronal view, dashed line represents the full outline of this broken tooth; **c**, UALVP 41, ceratopsian occlusal surface. Scale bar in (**a**) shows 1 cm blocks; scale bars in (**b**) and (**c**) are 1 cm. Abbreviations: ant, anterior; ce, cementum; cp, coronoid process; dent, dentary; db, dental battery; en, enamel; l, left; ling, lingual; os, occlusal surface; pdent, predentary; r, right.

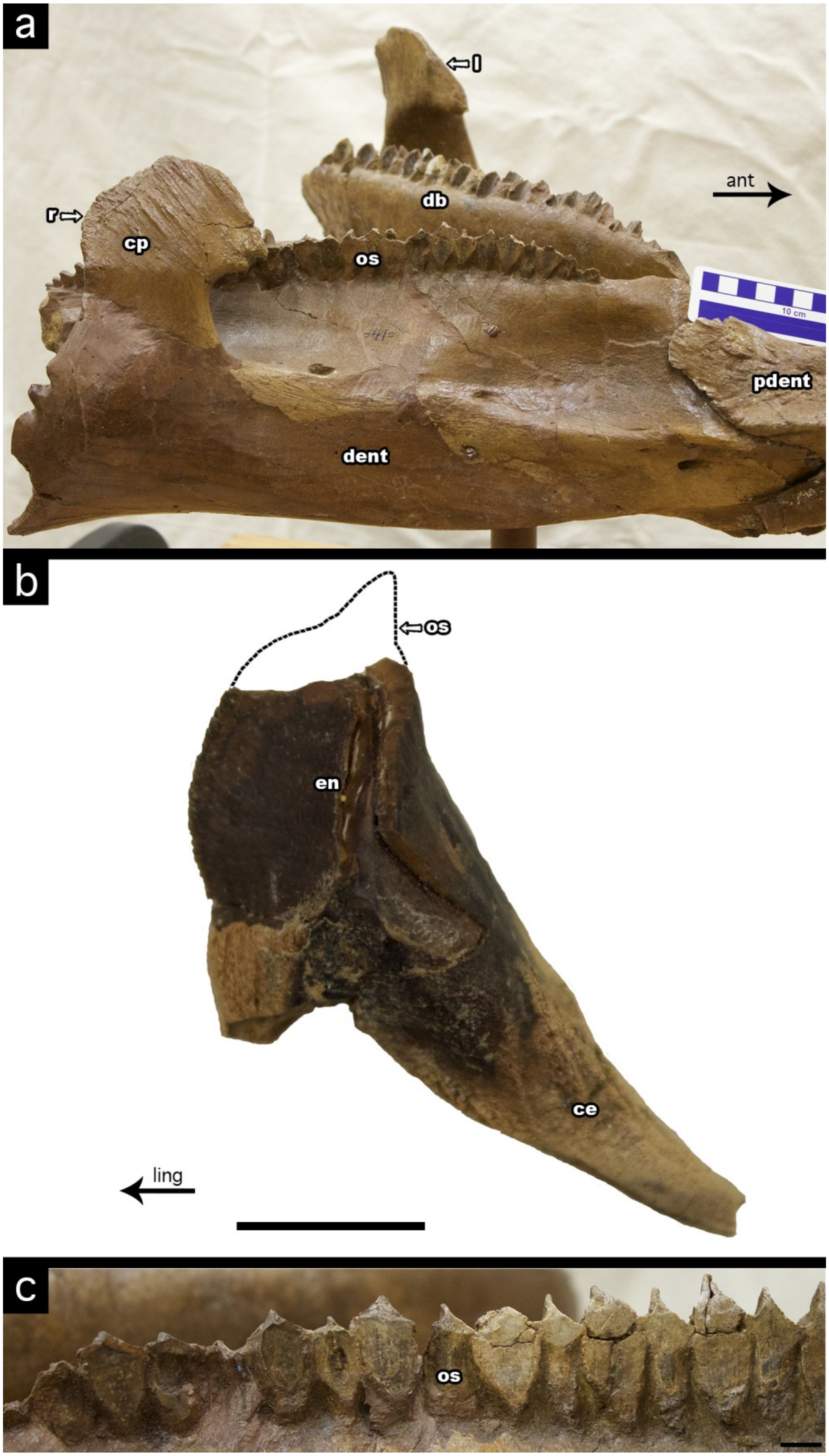
a
l
r
cp
db
os
ant
10 cm
pdent
dent
b
os
en
ce
ling
c
os

cause of their convergent evolution (Mallon and Anderson 2014). Nevertheless, the unique anatomy of the hadrosaur dental battery, which resulted in exceptional grinding abilities, is unlike anything known in extinct or extant herbivores.

1.3. The problems with studying the hadrosaurid dental battery

Despite our understanding of hadrosaurs, the mechanisms behind growth and development within the dental battery are still poorly understood. The dental battery has previously been considered a solid, robust structure with the interlocking teeth bound together by cementum (Cope 1883, Ostrom 1961, Erickson et al. 2012, Erickson and Zelenitsky 2014). If this was the case, how did tooth families become added to the dental battery? With adults having as many as 60 tooth families and nestlings having as few as six, there had to be a lot of growth and building of the dental battery throughout ontogeny. The ontogenetic changes that occurred within the dental battery as a result of this much growth need to be studied. No other vertebrate is known to add as many teeth during their ontogeny. As well, it would be beneficial to study the developmental processes of hadrosaurid dentine in order to fully understand the features seen in previous histological studies (Erickson et al. 2012, Erickson and Zelenitsky 2014).

In order to investigate these problems, histological sections were done of a perinatal and an adult dental battery. Extant analogues were also examined in an attempt to understand the soft tissues and developmental processes of the hadrosaurid dental battery. This study represents the first known histological study of an entire hadrosaurid dental battery in transverse view.

1.4. Introduction to the thesis chapters

Chapter 2 of this thesis focuses on the soft tissues of the dental battery and the tooth migration that occurs. The results of this chapter provide support for a ligamentous connection between teeth and challenge the established concepts about the dynamics of the hadrosaurid dental battery. An extant analogue for the soft tissue connections of hadrosaurid teeth is also introduced.

The next chapter focuses on the hard tissues, particularly dentine. The importance of using an appropriate extant analogue when trying to create hypotheses of developmental processes is discussed. This chapter also interprets a new type of hadrosaurid dentine, and provides justifications for the ontogenetic variation within the dentine of the hadrosaurid dental battery.

Chapter 2: Histological evidence for a dynamic dental battery in hadrosaurid dinosaurs with evidence of tooth migration

2.1 Introduction

Hadrosaurid dinosaurs were among the dominant megaherbivores of most Late Cretaceous ecosystems and likely owed this success to their specialized dentitions (Horner et al. 2004, Erickson et al. 2012, LeBlanc et al. 2016b). Their dentition was arranged in dental batteries, with up to 60 closely spaced vertical columns of diamond shaped teeth per jaw. Each column of teeth – a tooth family, sensu Edmund (1960) – was interlocked with the neighbouring tooth families and contained three to six successional teeth (Lull and Wright 1942, Horner et al. 2004). The crown-root angle of the dentary teeth, with respect to the occlusal surface, ranged from 120˚ to 140˚ in hadrosaurines and is greater than 145˚ in lambeosaurines (Horner et al. 2004). This angle permitted multiple teeth of each tooth family to be functional simultaneously (Lambe 1920, Ostrom 1961). Some species, such as *Edmontosaurus annectens*, had up to 60 tooth families with approximately 300 teeth per dentary (Lull and Wright 1942, Horner et al. 2004). This complex dental system increased the efficiency of grazing on tough vegetation, including siliceous phytoliths and the soil attached to low-lying vegetation (Tweet et al. 2008, Williams et al. 2009).

The hadrosaurid dental battery was originally considered to be a solid block with the crowns and roots of adjacent teeth being cemented together (Cope 1883, Ostrom 1961, Erickson et al. 2012). However, this view has been scrutinized more recently (LeBlanc et al. 2016b). Moreover, several histological studies have established homology of dental tissues and tooth attachment tissues between dinosaurs, mammals, and other archosaurs (Erickson et al. 2012, 2015, Erickson and Zelenitsky 2014, García and Zurriaguz 2015, Fong et al. 2016, LeBlanc et al.

2016a). Isolated teeth and portions of the hadrosaurid dental battery were thought to be bound together by cementum. Recent work, however has provided strong evidence that hadrosaurid dental batteries share the same tooth attachment tissues (alveolar bone, cementum, and periodontal ligament) as seen in other amniotes (LeBlanc and Reisz 2013, Fong et al. 2016, LeBlanc et al. 2016b). When all of these tissues are present, they provide a flexible connection between the tooth and its socket, a feature that LeBlanc et al. (2016b) extended to the complex dental batteries of hadrosaurids

The traditional model of a rigid dental battery with teeth cemented together (Cope 1883, Ostrom 1961, Erickson et al. 2012) fails to explain the problem of ontogenetic addition of tooth families and constant eruption that must have occurred in hadrosaurids. The dental battery must have been a dynamic structure, adding over 30 tooth families and undergoing constant tooth wear and replacement (Erickson 1996). However, the mechanisms of this movement are not well understood. According to the recent model of LeBlanc et al. (2016b) periodontal ligaments would mediate tooth eruption. Therefore, confirming their presence in hadrosaurids would provide support for the dynamic tooth battery model.

To test the traditional and recent models, the first known histological thin sections of an entire adult dental battery, as well as a nearly complete perinatal dental battery, were prepared along the occlusal (transverse) plane. If the dental battery was a rigid structure, cementum, or another hard tissue, should be found between the teeth. However, if the teeth were separated by sediment-filled spaces, this would suggest that periodontal ligaments, which mediate tooth movement, held the dental batteries together (LeBlanc and Reisz 2013).

2.2 Materials and methods

Histological thin sections were made of two hadrosaurid dentary dental batteries from the Upper Cretaceous of Dinosaur Provincial Park, Alberta, Canada. All cuts were made using the Buehler IsoMet 1000 slow-speed wafer blade. The perinatal dentary (UALVP 54419) and adult dentary (UALVP 56336) were cut transversely in two serial sections (Figures 2.1, 2.2). The perinatal dentary was embedded in a mixture of Castolite AC crystal clear polyester resin and degassed in a vacuum chamber. The adult dentary was initially reinforced at any weak points with Apoxie Sculpt self-hardening molding compound. The hardened resin blocks were then cut before and after the embedding process. All specimens were mounted to frosted plexiglass slides using either CA-40 bonding compound (UALVP 54419) or Polymer solutions PSI 122 resin and PSI 124 hardener (UALVP 56336) and cut away from the embedded portion. They were then ground down using a Hillquist thin section machine or a Crystal Master pro 12 lap wheel and further polished by hand using 600 and then 1000 grits of silicon carbide. These steps were repeated for the subsequent cuts of each dentary. The resulting thin sections were imaged using a Nikon DS-Fi-2 camera mounted to a Nikon AZ-100 microscope with NIS Elements BR imaging software (registered to D. C. Evans), or using a Nikon DS-Fi- 3 camera mounted to a Nikon Eclipse E600 POL microscope with NIS Elements D imaging software (registered to M. W. Caldwell).

A sagittal histological thin section of a modern rabbit (*Oryctolagus cuniculus;* UALVP 56918) lower incisor was made following the same protocol as the perinatal dentary. The incisor was first adhered to a basecoat of resin using CA-40 before being embedded to prevent the incisor from floating up during the degassing process in the vacuum chamber. For comparisons of tooth attachment in other archosaurs, previously made histological thin sections of a dentary of the extant crocodilian *Caiman sclerops* (made by Budney (2004)) were also examined. Images of the rabbit incisor and *C. sclerops* dentary thin sections were taken using a Nikon DS-Fi- 3 camera mounted to a Nikon Eclipse E600 POL microscope with NIS Elements D imaging software.

Figure 2. 1. The perinatal hadrosaurid right dentary (UALVP 54419). **a**, lingual and **b**, labial views of dentary before histological thin sectioning. Anterior is to the left in (**a**) and to the right in (**b**). The letters c and d in (**a**) correlate to images (**c**) and (**d**); **c**, occlusal transverse histological thin section; **d**, basal transverse histological thin section. Abbreviations: ant, anterior; bas, basal; ling, lingual; occl, occlusal; post, posterior.

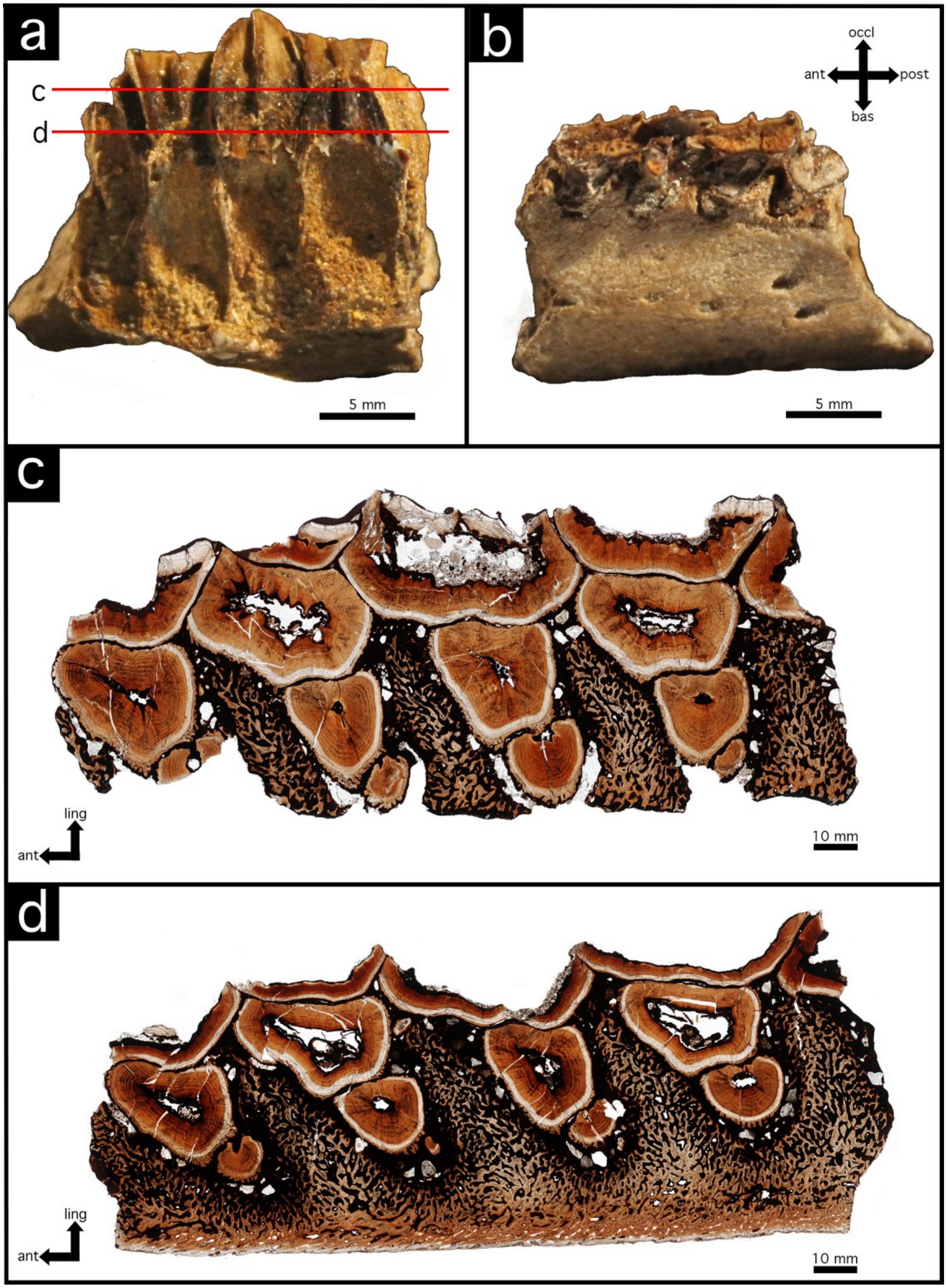
a
c
d
5 mm
b
occl
ant
post
bas
5 mm
c
ling
ant
10 mm
d
ling
ant
10 mm

Figure 2. 2. The adult hadrosaurid right dentary (UALVP 56336). **a**, lingual and **b**, labial views of dentary before histological thin sectioning. Anterior is to the left in (**a**) and to the right in (**b**). The letters c and d in (**a**) correlate to images (**c**) and (**d**); **c**, occlusal transverse histological thin section; **d**, basal transverse histological thin section. Abbreviations: ant, anterior; bas, basal; db, dental battery; jb, jaw bone; lab, labial; ling, lingual; occl, occlusal; os, occlusal surface; post, posterior.

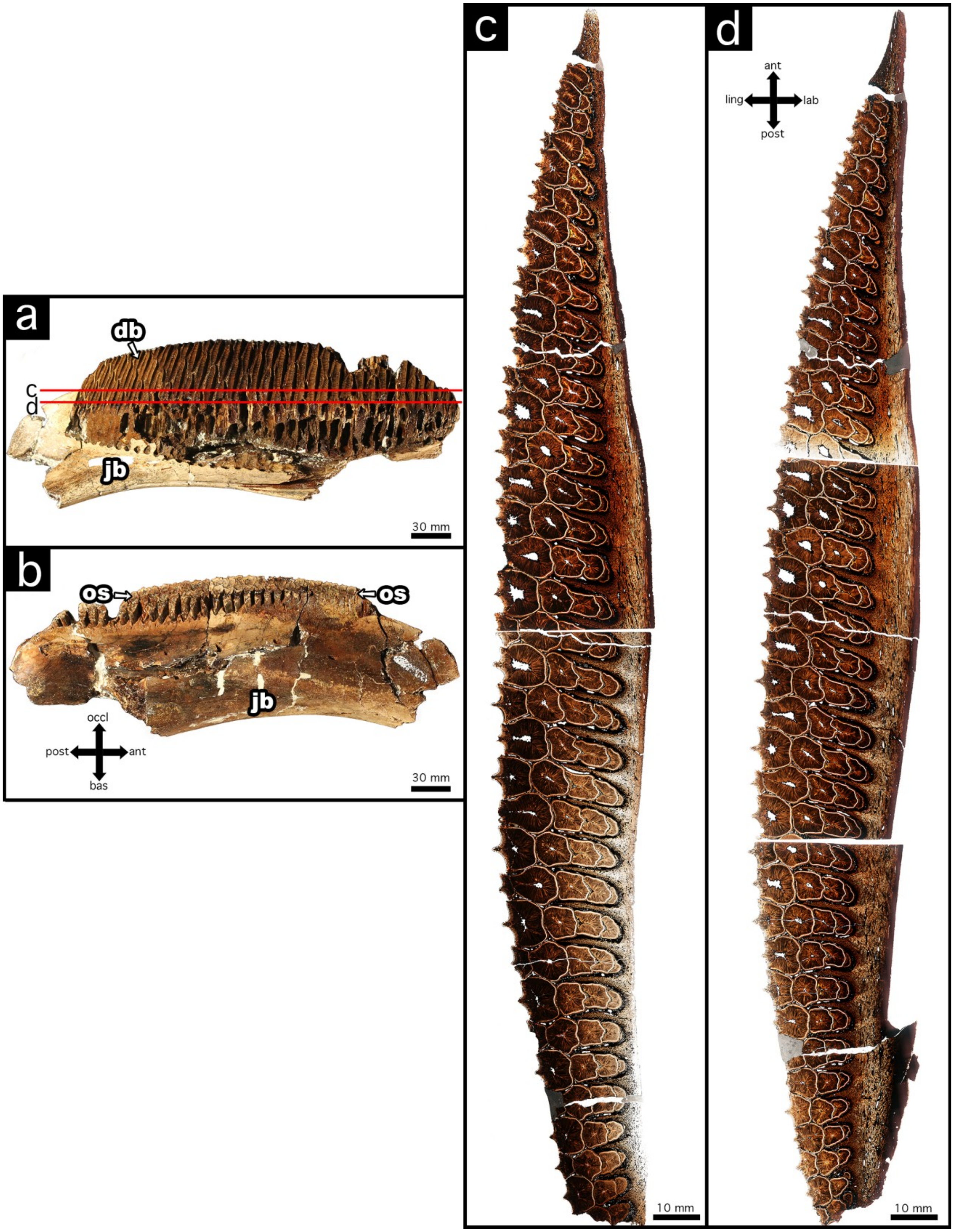
a
db
c
d
jb
30 mm
b
os
os
jb
occl
post
ant
bas
30 mm
c
10 mm
d
ant
ling
lab
post
10 mm

Angles of the alveolar septa were measured from the longitudinal axis of the jaw to the apex-base segment of the alveolar septum using ImageJ (Schneider et al. 2012). The tip-base segment is a line extending from the tip of the septum to the middle of the septum's base (Appendix 2.1, Fig. A-2.1).

Due to the unique structure of the hadrosaurid dental battery, typical dental terminology becomes ambiguous. For this reason anterior and posterior are used rather than mesial and distal, and labial and lingual are used to represent the part of the tooth closest to the cheek side and tongue side. For the two serial sections made of each dental battery, the occlusal thin section refers to the top thin section, closest to the occlusal surface, and the basal thin section refers to the lower thin section, closer to the base of the jaw. The term alveolar septum refers to the alveolar bone extending between tooth families.

2.3 Results

The perinatal dentary had five tooth families preserved with three or four teeth per family visible in the transverse sections, and only one tooth per family in occlusion (Figure 2.1). The adult dentary had 40 tooth families preserved with two to five teeth per family visible in transverse histological section and two to four teeth per family in occlusion (Figure 2.2).

2.3.1 Attachment Tissues

Thin sections of these dental batteries confirm the presence of three attachment tissues: cementum, periodontal ligament, and alveolar bone (Nanci 2013). These tissues are plesiomorphic for all amniote taxa histologically studied to date (Caldwell et al. 2003, Budney et al. 2006, Maxwell et al. 2011a, 2011b, LeBlanc and Reisz 2013, 2015, Pretto et al. 2014), and were first identified in the hadrosaurid dental battery by LeBlanc et al. (2016b)

Cementum is a mineralized connective tissue coating the tooth root that anchors the collagen fibers of the periodontal ligament (Gonçalves et al. 2005, Nanci 2013). Its two forms are acellular and cellular. The acellular cementum is a thin layer between the dentine and cellular cementum, whereas the cellular cementum is thicker with numerous cementocyte lacunae (Figure 2.3a, c). These tissues were arranged differently in hadrosaurs as the crown shifted from the top of the tooth to only the labial side (maxillary teeth) or lingual side (dentary teeth) (Lull and Wright 1942, LeBlanc et al. 2016b). The enamel covered one side of the diamond-shaped crown, whereas the cementum covered the remaining areas of the tooth (LeBlanc et al. 2016b). The layers of cementum seen in the thin sections do not come into contact with the cementum of adjacent teeth. Instead, a mineral-filled space is visible between every tooth position across and along the tooth families (Figure 2.3b, d). This pattern is seen throughout the entire dental battery (Figures 2.1, 2.2).

The sediment-filled space between every tooth probably once housed a network of periodontal ligaments. The periodontal ligament (PDL), a dense connective tissue, inserted into the cementum of the tooth root and attached the tooth to the alveolar bone of the jaw (Kraw and Enlow 1967, Nanci 2013). The portions of these collagen fibers (either partially or fully mineralized) embedded in the cementum and alveolar bone are termed Sharpey's fibers (LeBlanc and Reisz 2013, Nanci 2013). To illustrate, Figure 2.4 shows the PDL attachment in the extant crocodilian *Caiman sclerops*. Although the soft tissue of the PDL has long since decayed, the entire dental battery was clearly suspended by PDLs, and even individual teeth were connected to their neighbouring teeth by periodontal ligaments (LeBlanc et al. 2016b). In the thin sections, Sharpey's fibers are seen within the cementum for tooth-alveolar bone attachment as well as tooth-tooth attachment (Figure 2.3d, 2.5b). In some areas of the adult dental battery, where there is a junction between three teeth, PDL fibers probably attached to PDL fibers of adjacent teeth (Figure 2.3d). As shown by LeBlanc et al. (2016b), Sharpey's fibers can be seen directed towards partially resorbed teeth where the younger tooth attaches to the partially resorbed tooth via a thin layer of alveolar bone or repair cementum (Figure 2.7e).

Given the unique organization of hard tissues in hadrosaurids, where enamel was only on the lingual face of the dentary tooth (LeBlanc et al. 2016b) (Figure 2.3a), the PDLs could attach everywhere on the tooth except for the lingually facing enamel. Thus, there was PDL attachment throughout the dental battery, but no PDL attachment to the dentary lingual plate as the plate faces the enamel of the teeth (Figure 2.5d).

The ever-growing mammalian incisor shares this unique arrangement of dental hard tissues and is here proposed as an extant analogue to the condition in hadrosaurs. As in hadrosaurids, the enamel is restricted to one side of the tooth and cementum is surrounding the remaining sides of the tooth, as seen in a sagittal histological section of a rabbit (*Oryctolagus cuniculus*) mandibular incisor (Figure 2.5c). Sharpey's fibers are seen in great numbers on the lingual side of the tooth where the cementum covers the incisor (Figure 2.5a), whereas there are no Sharpey's fibers seen between the enamel-covered labial side of the tooth and the adjacent bone (Figure 2.5e). This has also been shown to be the condition for rodent incisors (Shellis and Berkovitz 1981, Stefen et al. 2016). This condition is similar in the hadrosaurid dentary, where Sharpey's fibers were entirely absent within the thin lingual plate, because this sheet of bone faced the enamel of the dental battery teeth and thus provided no sites for tooth attachment (Figure 2.5f).

Figure 2. 3. Attachment tissues in the hadrosaurid dental battery (UALVP 56336), all in transverse view. **a**, image of a whole tooth; **b**, a partial view of three tooth families; **c**, magnified image of the box in (**a**); **d**, magnified image of the box in (**b**). Abbreviations: ac, acellular cementum; cc, cellular cementum; de, dentine; en, enamel; pds, periodontal space; sf, Sharpey's fibers.

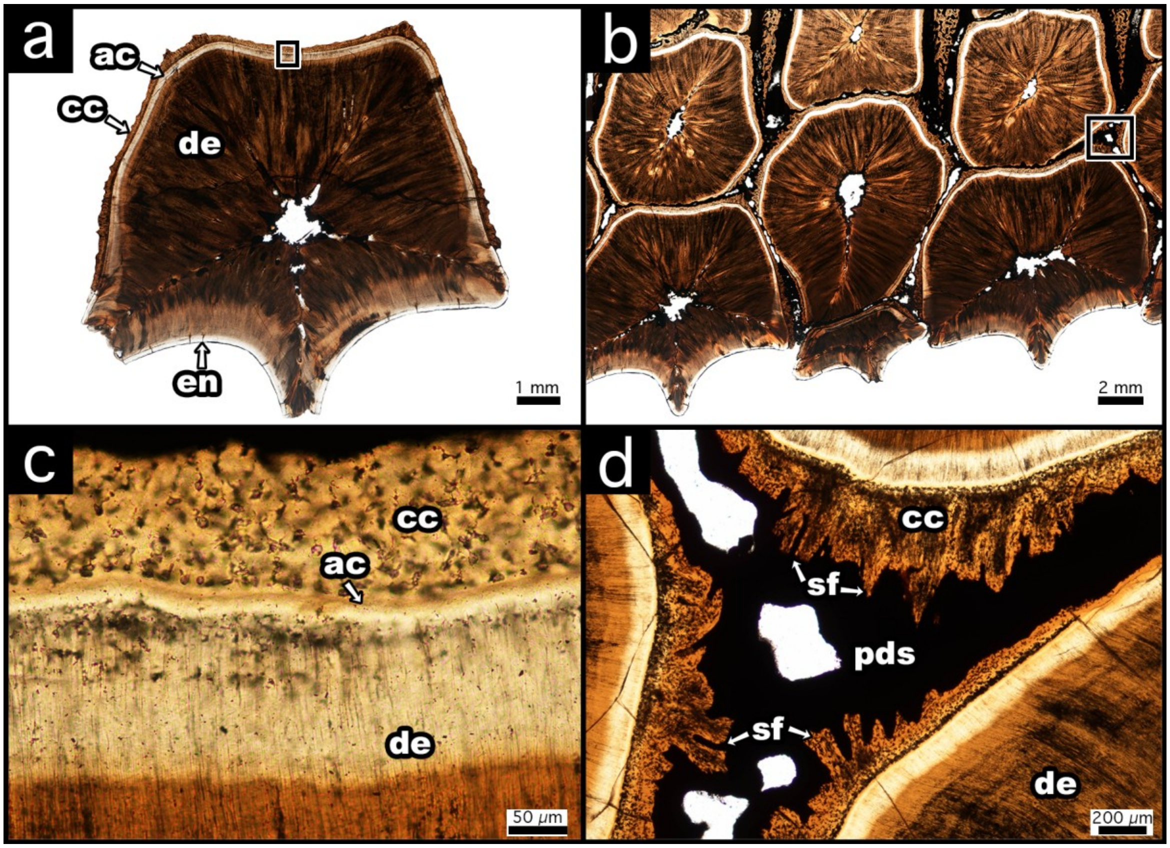
a
ac
cc
de
en
1 mm
b
2 mm
c
cc
ac
de
50 μm
d
cc
sf
pds
sf
de
200 μm

Figure 2. 4. Histological thin section of a *Caiman sclerops* tooth. **a**, image of tooth; **b**, magnified image of the box in (**a**). Abbreviations: ab, alveolar bone; c, cementum; de, dentine; pdl, periodontal ligaments.

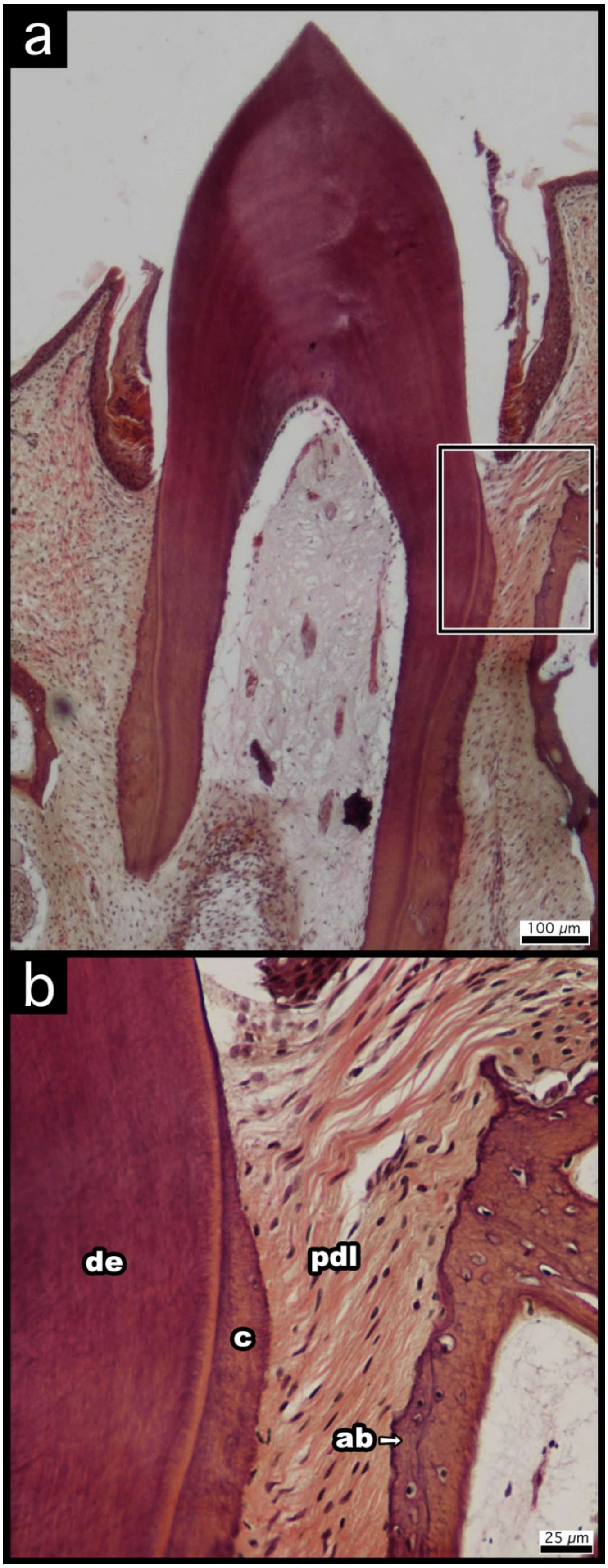
a
100 μm
b
de
pdl
c
ab→
25 μm

Figure 2. 5. Periodontal ligament attachment in the rabbit (*Oryctolagus cuniculus;* UALVP 56918) and hadrosaurid (UALVP 56336). **a**, magnified image view of the box in (**c**) of rabbit alveolar bone and the root portion of the incisor, sagittal view; **b**, corresponding view in the hadrosaurid dental battery between alveolar bone and the tooth root, transverse view; **c**, sagittal view of rabbit histological thin section; **d**, hadrosaurid dental battery (UALVP 11734) showing location of lingual plate [note: the lingual plate in this specimen is incomplete and would reach closer to the occlusal surface in life], medial view; **e**, magnified image of the box in (**c**) of rabbit alveolar bone and the crown portion of the incisor, sagittal view; **f**, corresponding view in the hadrosaurid dental battery between the lingual plate and the tooth crown (ROM 3500), coronal view. Abbreviations: ab, alveolar bone; c, cementum; de, dentine; en, enamel; lp, lingual plate; pcts, periodontal connective tissue space; pds, periodontal space; os, occlusal surface; sf, Sharpey's fibers. Image of ROM 3500 taken by A. LeBlanc, used with permission.

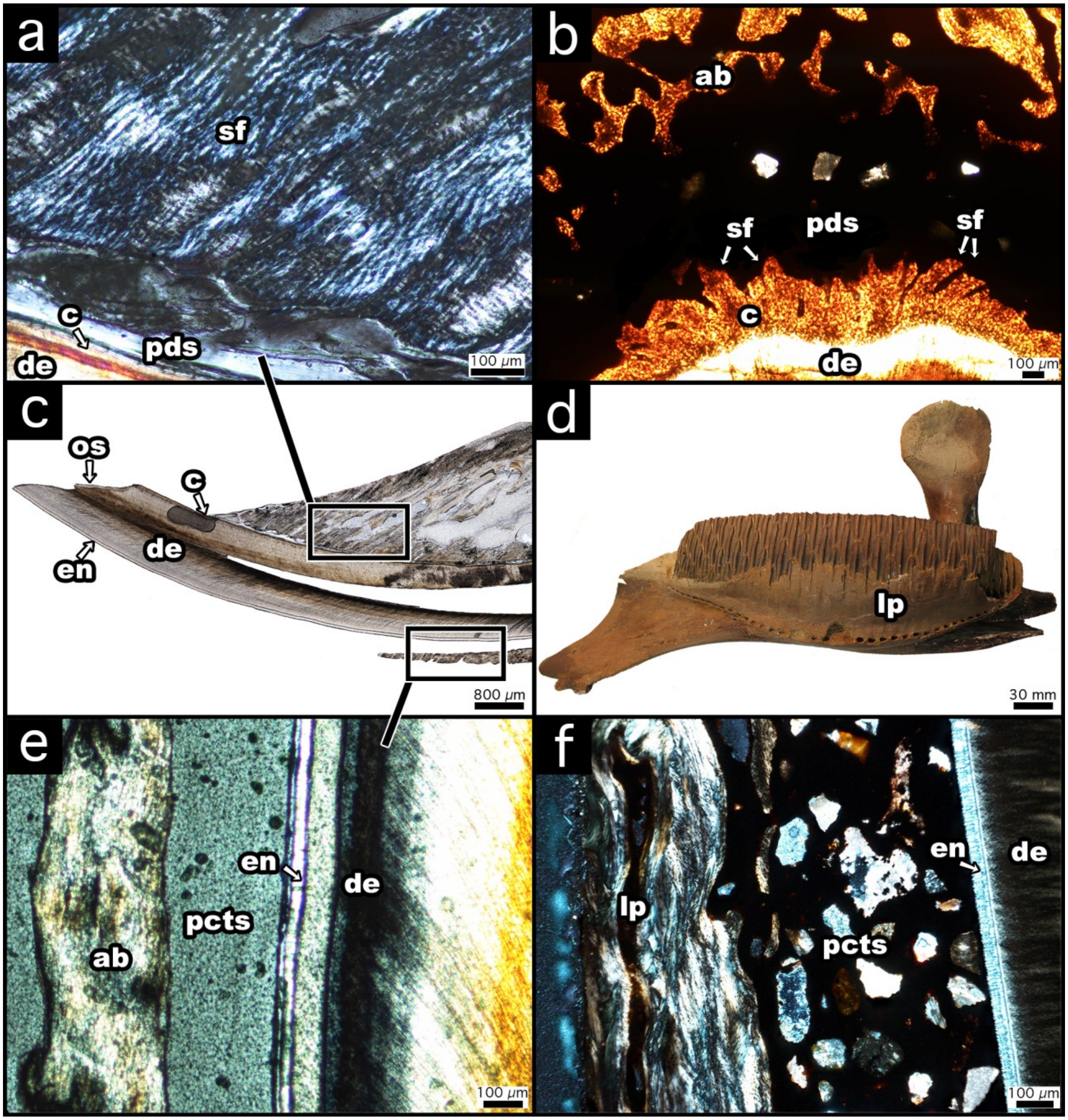
a
sf
c
pds
de
100 μm
b
ab
sf
pds
sf
c
de
100 μm
c
os
c
en
de
800 μm
d
lp
30 mm
e
en
de
pcts
ab
100 μm
f
en
de
lp
pcts
100 μm

2.3.2 Alveolar septa

Alveolar bone forms the tooth sockets and is composed of a quick growing, highly vascular, woven bone (Nanci 2013). This bone acts as a site of attachment for the Sharpey's fibers of the PDL (Caldwell et al. 2003, Nanci 2013). A reversal line (which defines the limit of bone resorption and where bone formation began) indicates the separation of the alveolar bone and the Haversian bone of the dentary in the adult specimen (Figure 2.6a). Alveolar septa are composed of alveolar bone and extend between tooth families, acting as partitions. These septa are wedge shaped, wide at the base, and narrowing towards the tip, and extend in between tooth families (Figure 2.6d, f, g, i). As the remodeling of the alveolar septa varies throughout the adult dental battery, descriptions of these septa have been categorized into four gradational zones based on morphologic similarities (Figure 2.6b). Zones were delineated based on development of alveolar bone, signs of bone resorption and apposition, and transverse inclination of the septa relative to the long axis of the jaw ramus. As serial thin sections were created for the dentary, angles are provided for both the occlusal and basal thin sections. The following zone descriptions are of the adult dentary.

Zone 1: Anterior zone. The first four anterior alveolar septa do not exist as proper partitions because no alveolar bone extends between the tooth families (Figure 2.6c). The first of these septa is not visible, but subsequent ones begin to swell and extend between the tooth families as they progress posteriorly through the alveoli. Alveolar bone on the anterior sides of the septa purportedly has irregular shallow troughs called Howship's Lacunae. These are created by osteoclasts as they resorb bone (Nanci 2013). There does not appear to be vascular bone trabeculae visible as these septa are composed mostly of older, thicker alveolar bone. The vascularity of these alveolar septa is high. The average angle of the alveolar septa in this zone (with the exception of the first) is 102˚ towards the anterior (range: 101˚-105˚) for the occlusal thin section and 104˚ towards the anterior (range: 98˚-111˚) for the basal thin section.

Zone 2: Mid-anterior dentary zone. The next 15 alveolar septa of the adult dentary extend between the tooth families towards the lingual plate (Figure 2.6d). The alveolar septa become longer and extend farther as they progress towards the middle of the battery. The anterior sides of these wedges show signs of new bone growth as they are lined with the thin woven bone trabeculae at the base of the septa and towards the tip. The posterior sides of these wedges have thicker compact lamellar bone with signs of being scalloped by purported Howship's lacunae (Figure 2.6e). These alveolar septa are generally less vascular than in the previous zone. The first four alveolar septa of this zone are highly angular, ranging from 122˚-125˚ for the occlusal thin section and 125˚-130˚ for the basal thin section, whereas the remaining 11 alveolar septa have an average angle of 107˚ for the occlusal cut and 111˚ for the basal thin section.

Zone 3: Mid-posterior dentary zone. The next 11 alveolar septa vary from those in the previous zones based on the presence of the newer, thin trabecular bone on both the posterior and anterior sides of the alveolar septa (Figure 2.6f). On the posterior surface, it is located at the base of the septum and not towards the tip. The amount of growth on the anterior surface varies throughout this zone, but there are always signs of newly forming bone. Halfway through this zone, the tips of the alveolar septa rotate towards the posterior. However, the overall alveolar septum remains anterior facing. The average angle of the alveolar septa in this zone is 99˚ towards the anterior (range: 91˚-105˚) for the occlusal thin section and 102˚ towards the anterior (range: 99˚-108˚) for the basal transverse section.

Zone 4: Posterior zone. The remaining visible alveolar septa angle posteriorly (Figure 2.6g), and all are inclined 90˚ or less towards the posterior. These alveolar septa still have new bone forming on the anterior sides of the septa, as well as on the posterior. The final few alveolar septa do not fully extend between the tooth families, similar to those of the first few anterior alveolar septa. The average angle of the alveolar septa in this zone is 80˚ – now angled posteriorly – (range: 68˚-88˚) for the occlusal thin section and 77˚ (range: 66˚-90˚) for the basal thin section.

In the perinatal dental battery, all of the alveolar septa are angled anteriorly. New bone growth is seen on all sides of the alveolar septa (Figure 2.6i), signifying rapid growth in all directions. The alveolar septa of the perinatal dental battery are relatively wider between tooth families than in the adult and consist entirely of a heavily vascularized woven bone matrix. However, the septa become more vascular towards the anterior end of the dental battery. The average angle of all alveolar septa is 111.2˚ towards the anterior (range: 103˚-118˚) for the occlusal thin section and 123.6˚ towards the anterior (range: 112˚-131˚) for the basal thin section.

2.3.3 Tooth resorption

Anterior teeth of the adult dental battery show signs of extensive resorption by neighbouring teeth (Figure 2.7a). Typically, resorption of older teeth by adjacent younger generations is roughly symmetrical (Figure 2.7b) as new teeth are forming on both sides of the older tooth. Symmetrical tooth resorption is caused by the development of newer teeth in the adjacent tooth families (LeBlanc et al. 2016b). This level of tooth resorption is highly uncommon in other vertebrates, as it would cause teeth to be shed (Edmund 1960), something the hadrosaurid dental battery avoids by the arrangement of hard tissues and the closely interlocking of tooth families held in place by the PDL. This asymmetrical scalloping of hadrosaurid teeth is not pathological, because the presence of Sharpey's fibers along these resorption surfaces indicates a PDL

Figure 2. 6. Zones of alveolar bone within the adult (UALVP 56336) and perinatal (54419) hadrosaurid dental batteries, all in transverse view. **a**, the junction between the bone of the jaw and the alveolar bone; **b**, whole section of the adult dental battery; **c**, magnified image of Zone 1; **d**, magnified image of Zone 2; **e**, magnified image of the box in (**d**); **f**, magnified image of Zone 3; **g**, magnified image of Zone 4; **h**, whole section of the perinatal dental battery; **i**, magnified view of the box in (**h**). Black arrows indicate direction of net movement of alveolar septum. (**c**), (**d**), (**e**), (**f**), and (**g**) are 90˚ counterclockwise to (**b**), while (**i**) is 90˚ counterclockwise to (**h**). Abbreviations: ab, alveolar bone; ant, anterior; as, apposition side; hl, Howship's lacunae; jb, jawbone; ling, lingual; post, posterior; rl, reversal line; rs, resorbing side.

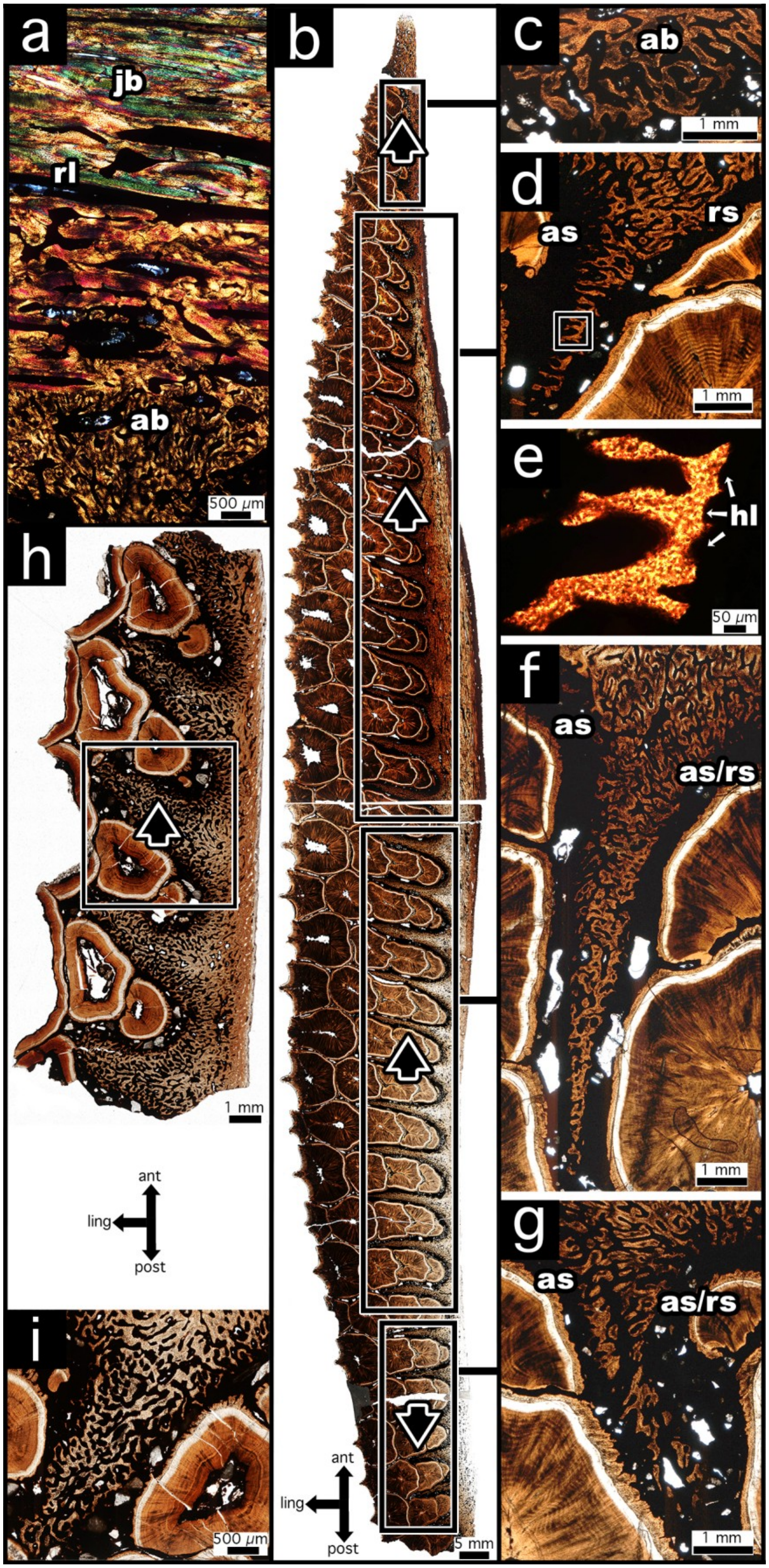
a
jb
rl
ab
500 µm
b
c
ab
1 mm
d
as
rs
1 mm
e
hl
50 µm
f
as
as/rs
1 mm
g
as
as/rs
1 mm
h
1 mm
ant
ling
post
i
500 µm
ant
ling
post
5 mm

connection remains between the teeth. Tooth resorption is further indicated by the presence of Howship's lacunae and a reversal line between the dentine of the partially resorbed tooth and the new layer of bone or repair cementum containing the Sharpey's fibers (Figure 2.7c).

The first tooth in the dental battery is half resorbed (Figure 2.7d). The tooth still retains a connection to the adjacent tooth via the PDL as evidenced by the uniform spacing and signs of Sharpey's fibers in cross-polarized light (Figure 2.7e). The adjacent tooth also shows signs of resorption anteriorly, indicating that the tooth is in natural position, and was not displaced postmortem.

2.4 Discussion

Tooth migration is the process of tooth positions drifting within the jaw either during growth or as a way to maintain tooth contacts as the teeth are worn by an abrasive diet (Kraw and Enlow 1967, Saffar et al. 1997). When a force is applied to a tooth, causing it to drift, the tooth is surrounded by areas of alveolar bone remodeling. The area of the tooth socket being remodeled by the direction of movement is the resorbing side (Kraw and Enlow 1967, Saffar et al. 1997). On this side of the socket, osteoclasts resorb the alveolar bone and all mineralized material, detaching the PDL from its anchorage to the alveolar bone (Kraw and Enlow 1967, Saffar et al. 1997). However, this resorption happens in asynchronous cycles where only a small proportion of the bone is being resorbed at one time, thus allowing a high percentage of PDLs of the tooth socket to maintain anchorage throughout migration (Saffar et al. 1997). Opposite to the resorbing side is the apposition side, where new bone is laid down by osteoblasts (Kraw and Enlow 1967, Saffar et al. 1997). This new alveolar bone appears thin and delicate as it consists of woven bone trabeculae and large vascular canals (Fong et al. 2016). The bone balance around the socket is always in equilibrium as the bone loss on the resorbing side is equal to the bone gain on the

Figure 2. 7. Tooth resorption in the hadrosaurid dental battery (UALVP 56336), all in transverse view. **a**, an asymmetrically resorbed tooth; **b**, a symmetrically resorbed tooth; **c**, magnified view of asymmetrically resorbed tooth; **d**, half resorbed tooth; **e**, magnified image of the box in (**d**). Black arrows indicate direction of resorption. Abbreviations: ab/rc, alveolar bone or repair cementum; ac, acellular cementum; cc, cellular cementum; cpc, collapsed pulp cavity; de, dentine; en, enamel; pds, periodontal space; rl, reversal line; sf, Sharpey's fiber.

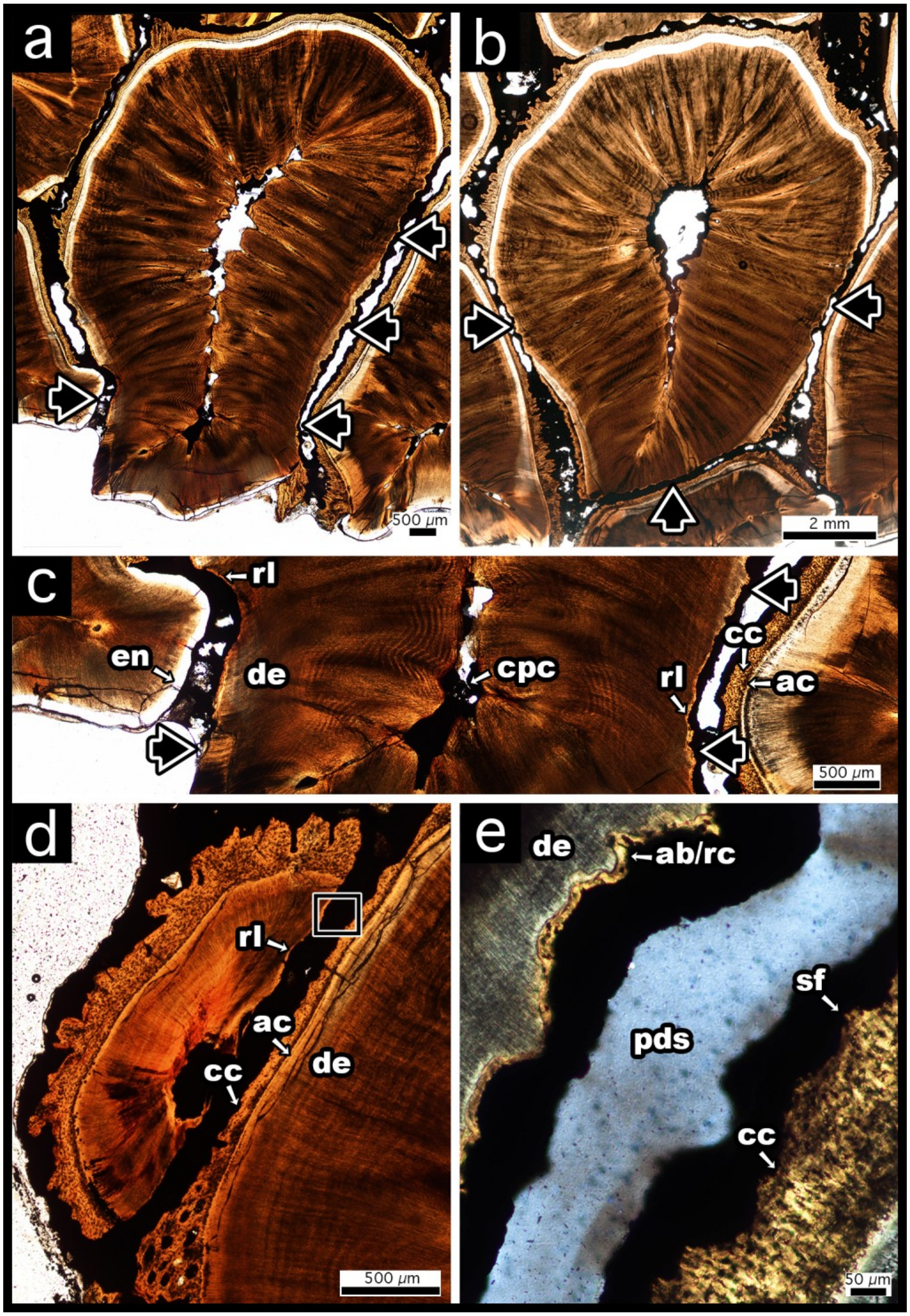
a
500 μm
b
2 mm
c
rl
en
de
cpc
rl
cc
ac
500 μm
d
rl
ac
cc
de
500 μm
e
de
ab/rc
pds
sf
cc
50 μm

apposition side (Vignery and Baron 1980, Saffar et al. 1997). While the migration rate decreases after growth, it never ceases completely (Kraw and Enlow 1967, Saffar et al. 1997).

Not all dinosaurian taxa with relatively complex dentitions show evidence of tooth migration. Recent CT work on sauropod dentition has provided examples of how alveolar septa are oriented between relatively stable tooth positions and little movement is seen in these alveolar septa except for when teeth enlarge as they migrate labially (Schwarz et al. 2015). These alveolar septa, particularly in the premaxilla, show no evidence of mediolateral movement other than what is required to enlarge the alveolus as the teeth grow in diameter. This creates a model for alveolar septa with zero net movement to which the hadrosaurid tooth migration can be compared. Multiple lines of evidence show tooth migration is occurring in the hadrosaurid dental battery, which is seen through the extensive remodeling of the alveolar bone, asymmetrical resorption of teeth, and from the displacement of successive generations of teeth.

Alveolar bone is formed of trabecular bone that later becomes more compact as lamellar bone fills in the trabecular spaces (Reid 1996). Migration of a tooth causes the adjacent alveolar bone to remodel as a result of resorption in the direction of tooth movement, and equal amounts of bone apposition on the opposite side (Kraw and Enlow 1967, Vignery and Baron 1980, Saffar et al. 1997). This zone of apposition and deposition is seen in most alveolar septa within the adult hadrosaurid dental battery. The apposition side of the alveolus has thicker bone trabeculae as bone has been deposited around the vascular spaces (Figure 2.6d), representing older, well-developed bone. The opposing side has thin vascular bone trabeculae (Figure 2.6d), representing new bone (Fong et al. 2016). When the area of bone apposition is on the posterior half of the alveolus, the direction of movement is directed anteriorly, and vice versa (Saffar et al. 1997).

The lack of alveolar septa reaching between the teeth in Zone 1 gives further evidence of soft tissues being responsible for holding the teeth together within the battery. The morphology of the alveolar septa in Zone 1 suggests there is a greater force moving these tooth families towards the anterior. In Zone 2 there is still a force pushing the tooth families forward; however the alveoli become less anteriorly angled towards the posterior limits of the zone. The alveolar septa of Zone 3 continue to become less angled anteriorly, but the newer, thin trabecular alveolar bone is visible on the posterior side of the alveolar septa. Finally, in Zone 4, the alveolar septa are angled posteriorly. Looking at the tooth migration of the dentary dental battery, there is a strong anterior force being applied to the anterior half of the dental battery, whereas it becomes weaker or changes direction towards the posterior of the dentary battery. However, in the perinatal dental battery all of the alveolar septa are angled anteriorly, suggesting that tooth migration begins early in ontogeny and that the posterior migration happens later in ontogeny. Both the adult and perinatal dental batteries show an increase of angularity in the alveolar septa deeper in thin section.

Tooth migration can also be observed by comparing the positions of successive tooth generations. As new teeth are added to the tooth families, there is an evident move towards the anterior (Zones 1-3; Figure 2.2c, d) or posterior (Zone 4; Figure 2.2c, d), as the newer tooth generations do not form a straight line with the older generations. This suggests that tooth migration is taking place between the additions of new tooth generations; otherwise the tooth families would have no angle to them.

Moreover, tooth resorption in the first few tooth families of the adult dentary is extensive on the posterior side of the tooth (Figure 2.3a). This further indicates tooth migration anteriorly. If there were no tooth migration occurring, the tooth resorption would be symmetrical as the younger teeth form in the adjacent tooth families. This asymmetrical resorption pattern is seen in only the most anterior tooth families, suggesting the anteriorly directed migration is stronger at the front of the dental battery. This level of asymmetric tooth resorption is not seen in the perinatal dental battery.

According to Gillette (from Edmund (1960), p. 174), tooth families can be lost in areas of the greatest crowding as successive teeth become larger. However, new tooth families being added to the jaw outnumbers those being lost from crowding. While Gillette was referring to the ankylosed teeth of a frog (*Rana pipiens*), this could still be relevant to a species exhibiting gomphosis, such as hadrosaurs. The half tooth at the beginning of the dental battery potentially represents a tooth family in the process of being lost if it was unable to migrate further anterior to make room for the adjacent drifting tooth family. As a result, the adjacent tooth family is partially overlapping the anterior tooth position.

The overall pattern of tooth migration shows how dynamic the hadrosaurid dental battery really is. There is not one, but multiple directions of migration within the dental battery as the teeth react to forces applied unequally throughout the dental battery via their PDL connections. Although the mechanisms behind tooth migration in the hadrosaurid dental battery require further investigation, opposition of forces during palinal mastication (Nabavizadeh 2014) may have had a strong influence. Regardless of the reason, the degree of movement within the dental battery is only possible due to the presence of a complex network of ligamentous connections between the teeth as well as between the teeth and alveolar bone. None of this could happen if a hard tissue, such as cementum, bound the teeth together.

Addition of tooth families is difficult to assess from the external view of the dental battery. Horner and Currie (Horner and Currie 1994) suggest the new tooth families are added to the front (Zone 1) and back (Zone 4) of the dental battery, because those teeth are smaller than the ones in the middle. Whereas the size of teeth might signify their age in some vertebrates (larger teeth replacing smaller ones) (Edmund 1960), there is nothing to suggest this is the case for hadrosaurids. Hadrosaurs may simply exhibit size heterodonty in teeth.

An alternative hypothesis is that tooth families are initially added on the posterior end of the dental battery, given the anterior orientation of all alveolar septa in the perinatal specimen. Tooth families do not appear to be added to the front of the larger battery as the alveolar septa and younger tooth generations are migrating towards the anterior. If tooth families were being added here, it would be predicted that alveolar septa and younger tooth generations would be migrating posteriorly to accommodate. Tooth families could have potentially been added to the posterior of the dental battery, but after the dental battery finished growing, the effects of the forces of occlusion erased all evidence of the newer tooth families. It should be noted that these observations were based on the perinatal and adult dentaries. To explore this hypothesis further, additional histological sections of a juvenile or subadult dentary where the animal is still growing are required.

In hadrosaurids, teeth within the occlusal surface are constantly being worn down, and the eruption rate must equal the attrition rate, as it does in the mammalian ever-growing incisor (Michaeli et al. 1977, Shellis and Berkovitz 1981). The mammalian ever-growing incisor is therefore an excellent model for examining how dental attachment tissues support constant eruption in hadrosaurids. Tooth eruption is a complex issue, and while the exact mechanism of tooth eruption in the mammalian ever-growing incisor is still unknown, there are two leading theories, including cellular proliferation at the base of the tooth (Berkovitz 1981, Gomes et al. 2013) and tension from the periodontal ligament (Beertsen et al. 1974, Beertsen 1975, Berkovitz 1981, Beertsen and Hoeben 1987).

Mandibular incisors of the lagomorph (*Oryctolagus cuniculus*) bear enamel on the labial side and cementum on the lingual side (Figure 2.5c) (Hirschfeld et al. 1973, Shellis and Berkovitz

1981), with cementum overlapping the enamel on portions of the lateral surfaces (Hirschfeld et al. 1973). As seen in rabbit thin sections, PDLs only attach to the cementum and thus only attach to the labial and lateral sides of the lagomorph – and rodent – incisors (Shellis and Berkovitz 1981, Stefen et al. 2016). In the mammalian ever-growing incisors, these attachment tissues are constantly remodeled in order to support the continuous eruption and likely play a mechanical role in incisor eruption (Beertsen et al. 1974, Beertsen 1975, Berkovitz 1981, Beertsen and Hoeben 1987).

Whereas tooth root elongation is not considered to be required for tooth eruption to take place in mammals (Gowgiel 1961), it may help play a role in hadrosaurid tooth eruption, despite extensive root resorption from surrounding, younger teeth. Root elongation is prominent within hadrosaurid teeth and, along with the PDL, likely acted as a mechanism for tooth eruption. Each individual hadrosaurid tooth may have its own eruptive forces. However, the PDL allowed the entire dental battery to erupt as a single unit through this unique tooth-tooth connection (LeBlanc et al. 2016b).

Currently, only *Bison bison* (American bison) and *Equus caballus* (horse) teeth (teeth adapted to support grazing diets) have been proposed as analogues for the grinding dentition of hadrosaurids based on their crest supporting and abscess-preventing dental tissues, as well as the prevalence of coronal cementum (Erickson et al. 2012). These analogues were proposed based on isolated hadrosaurid teeth, which do not provide information regarding tooth-to-tooth or tooth-to-alveolar bone interactions. For example, histological thin sections of two hadrosaurid dental batteries show no evidence of cementum between the teeth (Figures 2.1, 2.2). This tissue is used to indicate the sophistication in mammalian teeth and was thought to bind hadrosaurid teeth together (Erickson et al. 2012). Instead, using histological thin sections of entire dental batteries, the mammalian ever-growing incisor is proposed as a more accurate model, due to similarities in:

(1) the arrangement of dental hard tissues; (2) the cutting-edge occlusal surface created from tissue hardness differences (Osborn 1969, Shellis and Berkovitz 1981); (3) PDL attachment of one side of the tooth to alveolar bone; (4) a lack of PDL attachment between the enamel and alveolar bone on the opposing side; (5) continuous tooth eruption, similar to the continuous erupting tooth family of the hadrosaurid dental battery.

Lastly, the results presented here explain the extreme variation in the state of preservation of hadrosaurid dental batteries observed in the field. Isolated hadrosaurid teeth are common, and so are edentulous jaws (Figure 2.8a, b), which support the soft tissue model. But, complete dental batteries can be found in the field (Figure 2.8c, d), and these would seem to go against the soft tissue model. However, when complete batteries are recovered in the field, such as UALVP 56336, it is now clear that the infilling of the periodontal space with sediment during the fossilization process packs the teeth together, preventing the teeth from shedding or falling out of the jaw post-mortem.

2.5 Conclusions

This study supports the work by LeBlanc et al. (2016b) in showing compelling evidence for soft tissue connections between all of the teeth within the hadrosaurid dental battery. Histological thin sections of full dental batteries, originally considered robust, solid structures, have revealed a high degree of movement within the dental battery through ontogeny. The hadrosaurid dental battery was a dynamic and fluid structure due to constant bone remodeling and the presence of PDLs. While the exact cause of tooth migration in the hadrosaurid dental battery is unknown, it could be the result of forces from multiple sources, such as accommodation of new tooth families, opposition of forces during mastication, and occlusal wear. Furthermore, the ever-growing mammalian incisor is a more accurate extant comparison to hadrosaurid teeth as they share the distinctive arrangement of hard tissues and attachment tissues.

Figure 2. 8. Hadrosaurid dentaries with and without teeth preserved. **a**, UALVP 54938 without teeth, white arrows indicate a few of the alveolar septa; **b**, UALVP 54812, histological thin section of a dental battery without teeth; **c**, UALVP 11734, a dentary with teeth; **d**, UALVP 56336, histological thin section of a dental battery with teeth. Abbreviations: ant, anterior; db, dental battery; lab, labial.

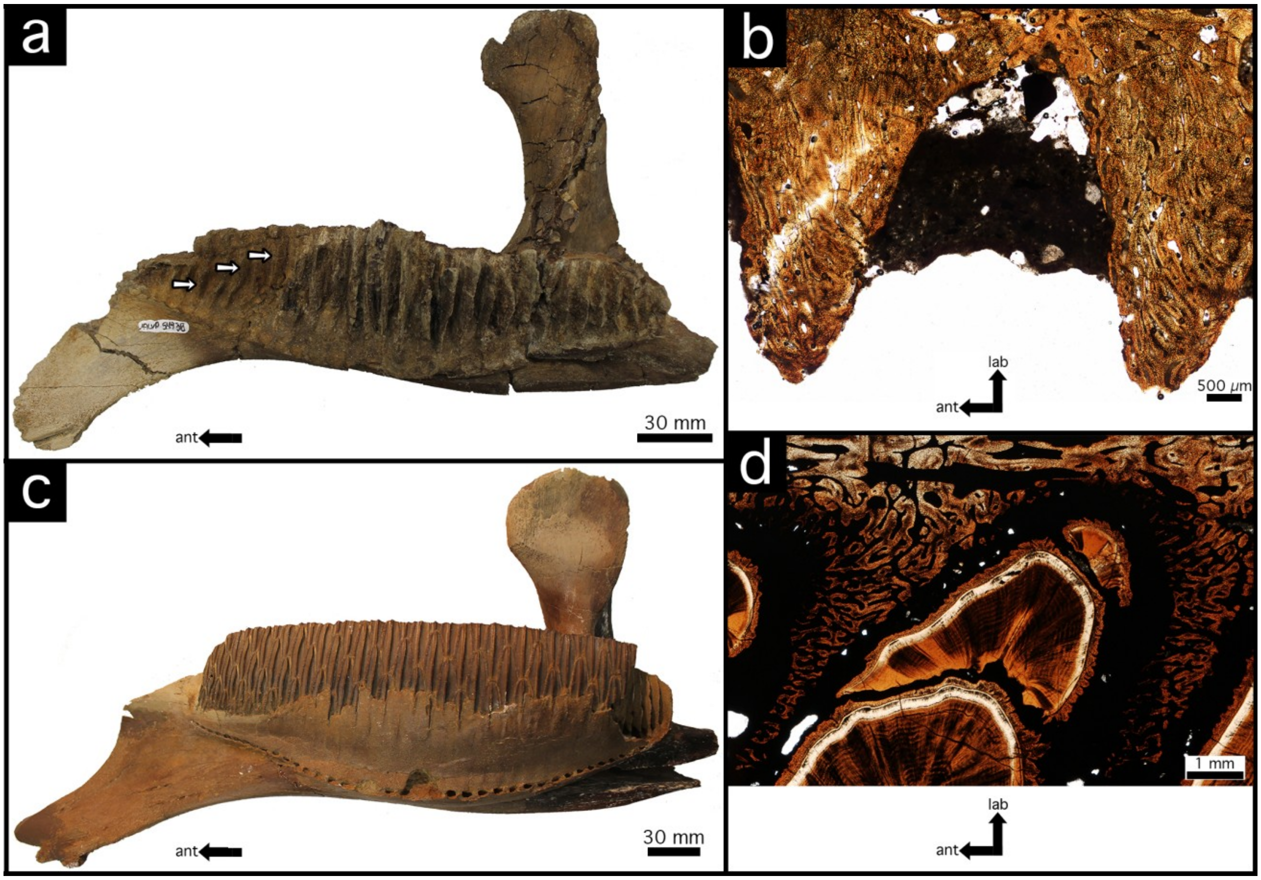
a
ant
30 mm
b
lab
ant
500 μm
c
ant
30 mm
d
1 mm
lab
ant

Appendix 2.1

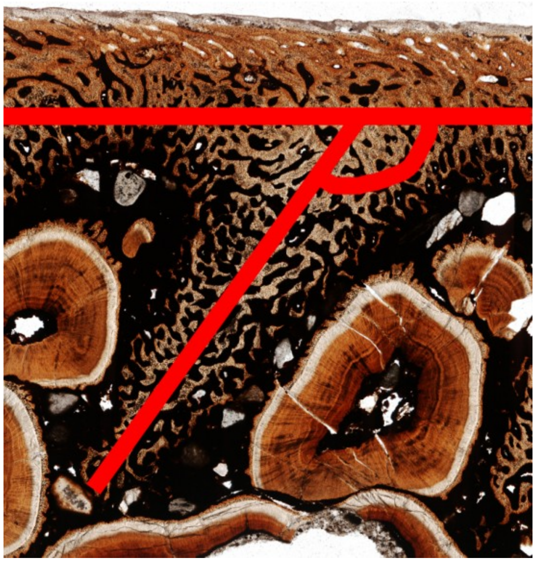

Figure A-2. 1. Visualization of the angles used for measuring the migration of alveolar septa. Anterior is to the left of the image.

Chapter 3: Using the mammalian ever-growing incisor as a model for dentinogenesis in the teeth of hadrosaurid dinosaurs

3.1 Introduction

Hadrosaurid dinosaurs were large herbivores that dominated most Late Cretaceous ecosystems. They likely owed their success to their dental battery, a specialized dental array with a complex organization of teeth (Horner et al. 2004). A dental battery is composed of multiple interlocked vertical stacks of teeth called tooth families (sensu Edmund (1960)) (Figure 3.1a). Hadrosaurid teeth, as in other amniotes, are composed of the hard tissues enamel, dentine, and cementum (Erickson et al. 2012, Erickson and Zelenitsky 2014, LeBlanc et al. 2016b). However, the enamel, the protective covering of the tooth crown (Nanci 2013), has an unusual distribution in hadrosaurids compared to most other amniotes, as it is only found on the labial sides of the maxillary teeth and on the lingual sides of dentary teeth (Figure 3.1b) (Lull and Wright 1942). This creates different patterns of functional enamel on the occlusal surfaces of the maxilla and dentary (Figure 3.1c, d, e). As in all other reptiles and mammals, orthodentine (hereafter referred to as dentine), which forms most of a hadrosaurid tooth, is composed of closely packed dentinal tubules (Nanci 2013). Dentine is typically separated into primary and secondary dentine. The outermost layer of the primary dentine is a thin atubular layer called mantle dentine, which borders the enamel and cementum (Osborn 1969, Jones and Boyde 1984, Erickson et al. 2012, Nanci 2013). The remaining primary dentine, circumpulpal dentine, forms the bulk of the tooth (Goldberg et al. 2011, Nanci 2013). After the tooth root has formed, secondary dentine deposition begins and slowly continues asymmetrically throughout the life of the tooth (Goldberg et al. 2011, Nanci 2013). The tubular structure of secondary dentine is typically continuous with that of

Figure 3. 1. The hadrosaurid dental battery and dentition. **a**, UALVP 11734, right dentary, lingual view, anterior is to the left; **b**, UALVP 55127, an isolated hadrosaurid dentary tooth, lingual (left) and coronal (right) views; **c**, occlusal view of a hadrosaurid left maxilla (UALVP 99), white arrows indicating the presence of enamel, anterior is to the left; **d**, occlusal view of a hadrosaurid right dentary (CMN 351), white arrows indicating the presence of enamel, anterior is to the right; **e**, coronal view of maxilla and dentary with each showing a cross section of a single tooth family, grey represents jaw bone, white represents teeth, black represents enamel. Abbreviations: ce, cementum; cej, cemento-enamel junction; db, dental battery; en, enamel; tf, tooth family.

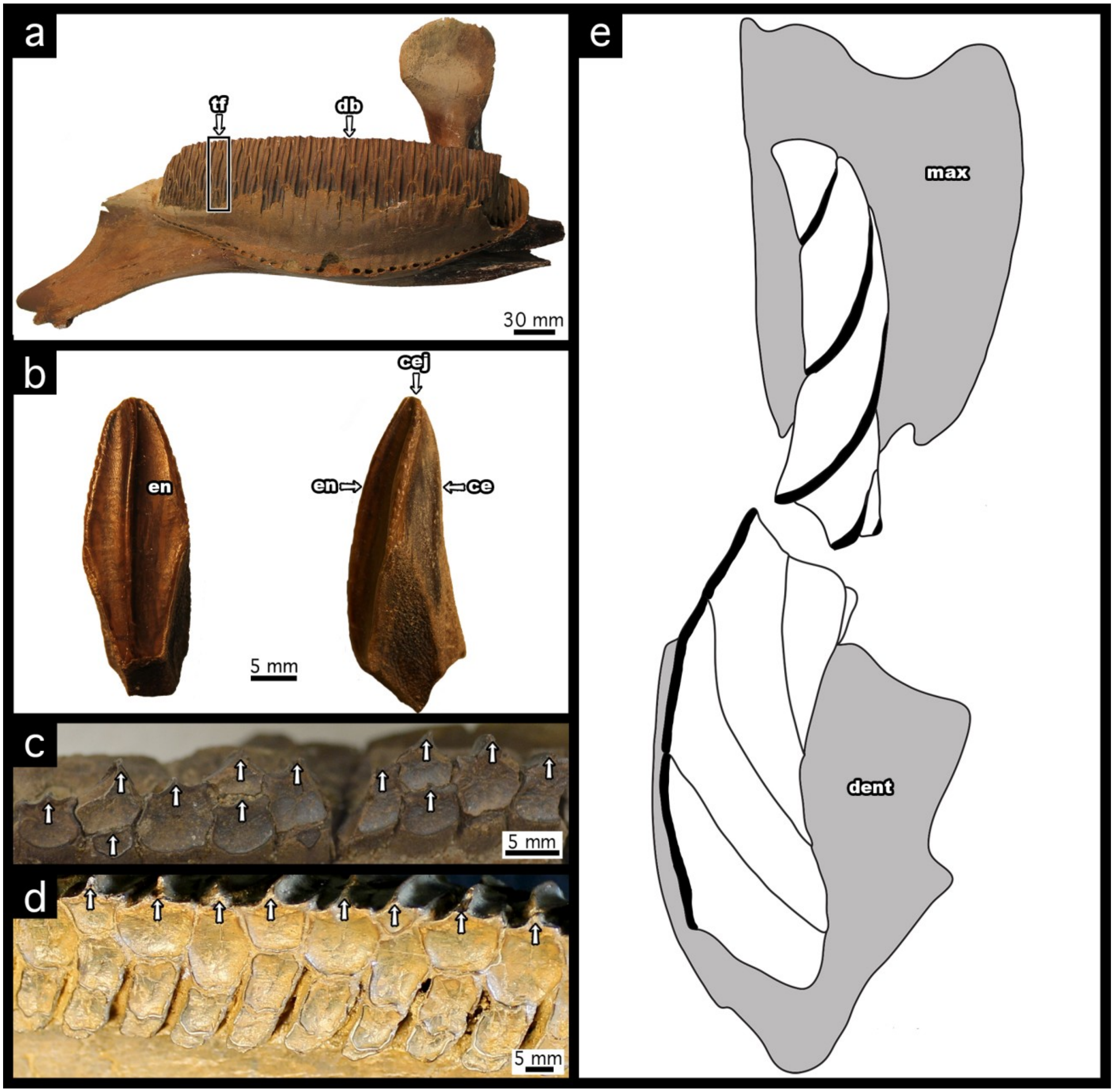
a
tf
db
30 mm
b
en
cej
en
ce
5 mm
c
5 mm
d
5 mm
e
max
dent

primary dentine, with only slight morphological differences separating the two dentine types (Goldberg et al. 2011, Nanci 2013). Based on histological examination of isolated hadrosaurid teeth, Erickson et al. (2012) suggested hadrosaurids developed new dentine types.

Erickson et al. (2012) proposed *Bison bison* (American bison) and *Equus* (horse) teeth as extant analogues for hadrosaurid teeth based on the presence of coronal cementum, secondary dentine, and crest-supporting tissues. These comparisons led them to argue that the complexity of hadrosaurid teeth rivals that of advanced herbivorous mammals (Erickson et al. 2012).Whereas the hadrosaurid dental battery as a whole is a complex structure with numerous crest and valley-forming tissues (Figure 3.1c, d), individual teeth are very different from those of modern ungulates. Hadrosaurid teeth actually show more structural similarities to mammalian ever-growing incisors, which have identical distributions of enamel, cementum, and dentine (Shellis and Berkovitz 1981, LeBlanc et al. 2016b).

The mammalian ever-growing incisor is seen in the Glires, a clade comprising rodents (beavers, mice, porcupines, rats, squirrels, etc.) and lagomorphs (hares, pikas, rabbits). One long, curved, incisor is positioned at the front of each jaw quadrant, with rabbits having an extra smaller incisor in the maxilla behind the primary incisor (Shellis and Berkovitz 1981). These incisors have enamel on the labial surface of the tooth, with the remaining surface covered by cementum (Shellis and Berkovitz 1981). With the enamel only on one side of the tooth, the softer dentine and cementum are worn away faster by the occluding incisor, forming a sharp chisel-like edge used for gnawing on a traditionally herbivorous diet (Shellis and Berkovitz 1981).

As the constantly erupting incisor grows rapidly to compensate for wear, it requires rapid dentinogenesis to prevent pulp cavity breaches at the occlusal surface as the tooth wears away. A similar process has been suggested to have occurred in hadrosaurid teeth (LeBlanc et al. 2016b). Given the similarity in tissue arrangement and function, the mammalian ever-growing incisor may provide important insights into dentinogenesis of the hadrosaurid tooth. For these reasons, the hard tissue arrangements and dentinogenesis in the ever-growing incisor are compared to those of individual hadrosaurid teeth in order to better understand the evolution and development of the hadrosaurid tooth.

3.2 Materials and methods

Serial transverse thin sections of the upper incisor of a beaver (*Castor canadensis*; UALVP 56917) and a sagittal histological thin section of the lower incisor of a modern rabbit (*Oryctolagus cuniculus;* UALVP 56918) were made (Appendix 3.1, Figs. A-3.1, A-3.2). Both incisors came from dry skulls. The incisors were first glued to a basecoat of resin using CA-40 before being embedded in a mixture of Castolite AC crystal clear polyester resin that was then degassed in a vacuum chamber. All cuts were made using a Buehler IsoMet 1000 slow-speed wafer blade. The specimens were mounted to frosted plexiglass slides using CA-40 bonding compound and cut away from the embedded portion. They were then ground down using a Hillquist thin section machine and further polished by hand using 600 and then 1000 grits of silicon carbide. These steps were repeated for the subsequent cuts of the beaver incisor. For comparison, previously made histological thin sections were examined of an incisor of a pika (*Ochotona* sp., from the histology slide collection of the Advanced Microscopy Facility, University of Alberta, cabinet 28 tray 19).

Histological thin sections were also made of two hadrosaurid dentary dental batteries from the Upper Cretaceous of Dinosaur Provincial Park, Alberta, Canada. The perinatal dentary (UALVP 54419) and adult dentary (UALVP 56336) were cut transversely in two serial sections (Appendix 3.1, Figs. A-3.3, A-3.4). The perinatal dentary was prepared using the same methods as the mammalian incisors, minus the use of a basecoat. The adult dentary was initially reinforced at any weak points with Apoxie Sculpt self-hardening molding compound. The hardened resin blocks were then cut before and after the embedding process. They were then mounted to frosted plexiglass slides using Polymer PSI 122 resin and PSI 124 hardener and cut away from the embedded portion. The adult dentary was then ground down using a Crystal Master pro 12 lap wheel and further polished by hand using 600 and then 1000 grits of silicon carbide. These steps were repeated for the subsequent cuts of the adult dentary

The resulting thin sections were imaged using a Nikon DS-Fi-2 camera mounted to a Nikon AZ-100 microscope with NIS Elements BR imaging software (registered to D. C. Evans), or using a Nikon DS-Fi- 3 camera mounted to a Nikon Eclipse E600 POL microscope with NIS Elements D imaging software (registered to M. W. Caldwell). Before thin sectioning, the beaver and rabbit incisors were imaged using a Q Imaging Retiga 4000R camera mounted to a Nikon SMZ1500 microscope with NIS Elements BR imaging software (registered to E. B. Koppelhus).

Due to the unique structure of the hadrosaurid dental battery, some dental terminology becomes ambiguous. For this reason anterior and posterior are used rather than mesial and distal, and labial and lingual are used to represent the parts of the tooth closest to the cheek side and tongue side.

3.3 Results

3.3.1 Hard tissues of the mammalian ever-growing incisor

Glires, a clade consisting of rodents and lagomorphs, have ever-growing incisors with enamel only on the labial side of each tooth and acellular cementum on the lingual side (Figure 3.2a, b, c). Each group exhibits different patterns of the prisms that comprise the enamel layer. For the lagomorphs, a leporid (hare or rabbit) has a single layer of Hunter-Schreger bands (HSB), where enamel prisms cross each other at right angles (Martin 2004). For rodents, as observed in the beaver thin sections, a double layer of enamel is seen – an inner layer with HSB and an outer layer of radial enamel (Figure 3.2d). In the radial enamel, prisms are arranged parallel to each other (Martin 1994). For rodent incisors, the thickness of the HSB has phylogenetic significance (von Koenigswald and Mörs 2001). The outer edge of the enamel in some rodents is also pigmented orange or brown with iron (Stein and Boyle 1959, Møinichen et al. 1996, Gordon et al. 2015) (Figure 3.2d). This iron-rich layer increases the hardness and acid resistance of the enamel (Stein and Boyle 1959, Møinichen et al. 1996, Gordon et al. 2015).

The dentine of the mammalian ever-growing incisor is generally round or oval in transverse view (Figure 3.2b), with enamel covering the labial surface and cementum covering the remaining surfaces. The pulp chamber is large at the base of the tooth and is closed and pinched off at the distal tip (Figure 3.3). Serial thin sections of the beaver incisor show this growth trajectory of the dentine, with the circumference of the pulp cavity decreasing towards the occlusal surface (Figure 3.3). This dentine is composed of three visually distinct layers. Mantle dentine is the outermost layer of primary dentine (Nanci 2013). Unfortunately, this dentine layer was not visible in the beaver and rabbit thin sections. This is likely because the ground thin sections were not stained. In stained thin sections, mantle dentine appears as a thin white band (Rosenberg and Simmons 1980). Internal to the mantle dentine are two salient bands of dentine, seen in both the beaver and rabbit thin sections (Figure 3.2e, f). Under the enamel, the first band is on average 41µm thick in the beaver and 35 µm thick in the rabbit. In the beaver this first band appears dark under plain polarized light, but is highly birefringent under cross-polarized light. In the rabbit, this band of dentine is light under plain polarized light and birefringent under cross-polarized light. The second band is on average 150 µm thick in the beaver and 162 µm thick in the rabbit. In the beaver, this second band appears light in plain polarized light and becomes birefringent under cross-polarized light. There is a sharp border between the two bands in the beaver (Figure 3.2e). In the rabbit, this second band is marginally darker than the first band under plain polarized light, but in cross-polarized light the birefringence is markedly darker than in the first band (Figure 3.2f). A birefringent band of dentine is also present at the cemento-dentine junction (CDJ), but not as prominently. These bands may be a result of differences in collagen fiber or calcospherite orientation, and can help differentiate dentine from other hard tissues like bone and cementum (Shellis 1981). Adjacent to these bands is the remaining primary dentine. The transverse thin sections of the beaver incisor reveal many concentric rings within the dentine known as lines of von Ebner, which represent hyper- and hypocalcified layers of dentine, purportedly representing daily growth rates (Rinaldi and Cole 2004) (Figure 3.2g). The average distance between these lines of von Ebner is 28 μm.

The growth of dentine in the mammalian ever-growing incisor moves from the perimeter of the tooth towards the pulp (Schour and Steadman 1935, Rosenberg and Simmons 1980, Steinfort et al. 1990). The odontoblast layer is pseudostratified, and is preceded by the pulp and succeeded by dentine (Figure 3.4). The pika thin sections revealed a highly vascular pulp cavity (Figure 3.4). The blood vessels are circular in cross section and extend in an apical-occlusal direction, with some transverse connections visible. Blood vessels range from 11μm to 67 μm in diameter in a thin section close to the base of the tooth, and from 12 μm to 170 μm in a thin section taken from slightly closer to the occlusal surface. Many fibroblasts are also seen throughout the pulp (Figure 3.4b). The blood vessels likely halt the advancement of some odontoblasts, creating an undulating boundary around the pulp cavity in thin section (Figure 3.2h).

Figure 3. 2. Histology of the mammalian ever-growing beaver (*Castor canadensis*; UALVP 56917) and rabbit (*Oryctolagus cuniculus*; 56918) incisors. **a**, cross-section of a beaver incisor, distal end, labial is to the right, lingual is to the left; **b**, beaver incisor, labial is to the bottom, lingual is to the top; **c**, the cemento-enamel junction, magnified image of box in (**b**), rotated 90˚ counterclockwise; **d**, enamel of the beaver; **e**, dentine banding in the beaver, in cross-polarized light; **f**, dentine banding in the rabbit, in cross-polarized light; **g**, concentric rings within the beaver dentine; **h**, undulating dentine growth in the beaver incisor. Images (**b-h**) in transverse view. Black brackets in (**a**), (**d**), (**e**), and (**f**) represent the extent of the areas the abbreviations indicate. Abbreviations: ac, acellular cementum; cej, cemento-enamel junction; de, dentine; deb1, dentine band 1; deb2, dentine band 2; en, enamel; hsb, Hunter-Schreger bands; os, occlusal surface; pc, pulp cavity; pi, pigmented enamel; re, radial enamel.

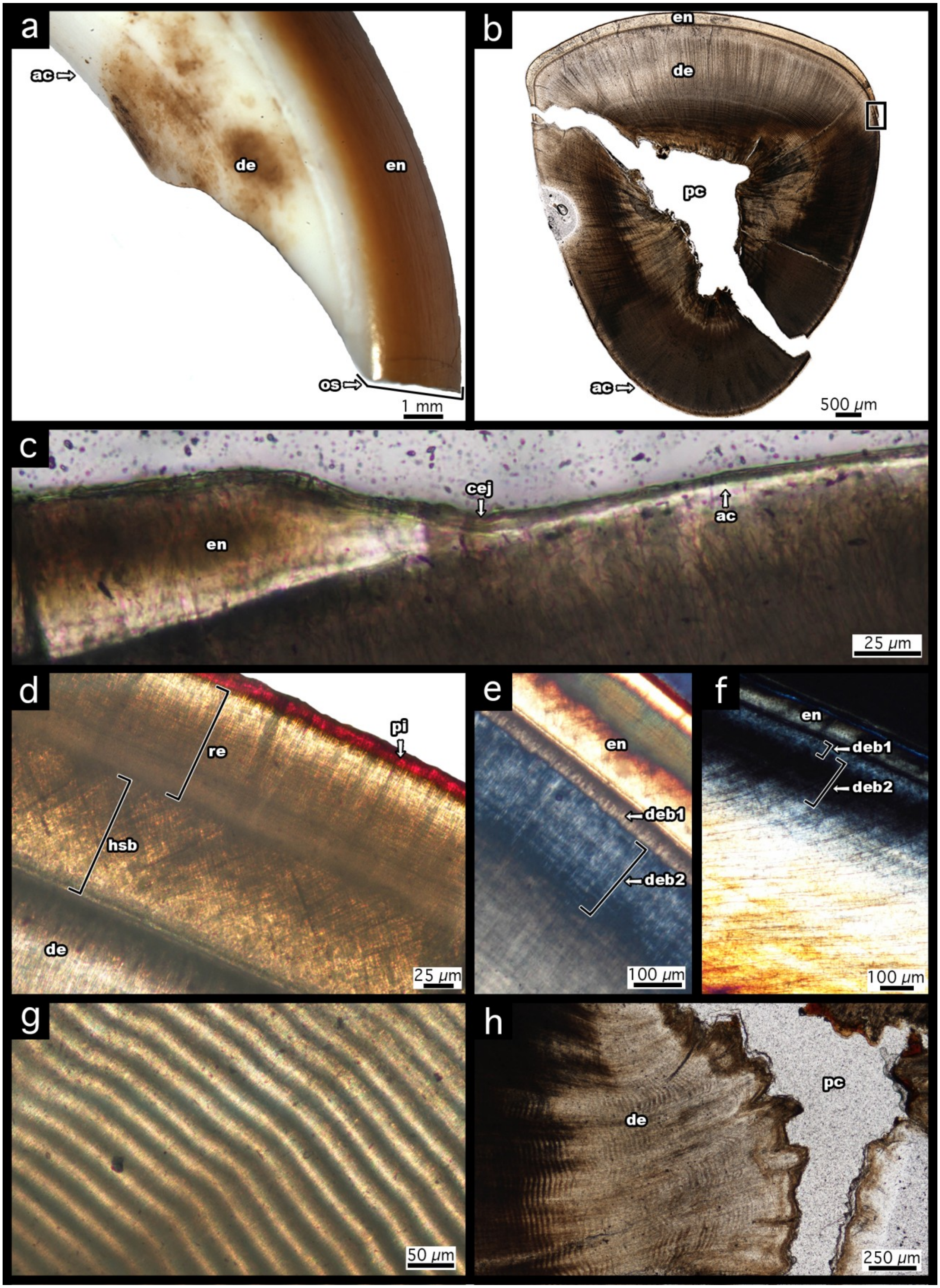
a
ac
de
en
os
1 mm
b
en
de
pc
ac
500 μm
c
cej
ac
en
25 μm
d
re
pi
hsb
de
25 μm
e
en
deb1
deb2
100 μm
f
en
deb1
deb2
100 μm
g
50 μm
h
pc
de
250 μm

Figure 3. 3. The pulp cavity of the mammalian ever-growing incisor. The rabbit incisor (*Oryctolagus cuniculus*; UALVP 56918) provides a sagittal view of a typical mammalian ever-growing incisor. Although a different species, the beaver thin sections (*Castor canadensis*; UALVP 56917) show the width of the pulp cavity in transverse view where it would correspond to the sagittal thin section, as indicated by the black lines. The sagittal and transverse thin sections provide a holistic view of the change of pulp cavity width between the base and distal tip of the mammalian ever-growing incisor. All scale bars are 500 µm. Abbreviations: de, cementum; de, dentine; en, enamel; pc, pulp cavity.

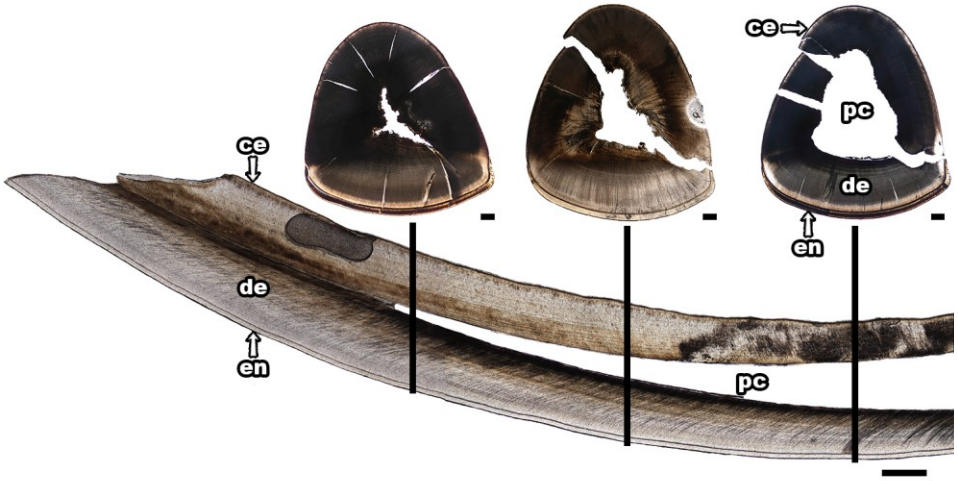
ce
pc
de
en
ce
de
en
pc

Figure 3. 4. Pika incisor (*Ochotona sp.*) transverse thin section. **a**, view of the thin section, labial is to the top of the image; **b**, magnified view of box in (**a**). Abbreviations: bv, blood vessel; de, dentine; es, enamel space; fi, fibroblast; od, odontoblast layer; p, pulp.

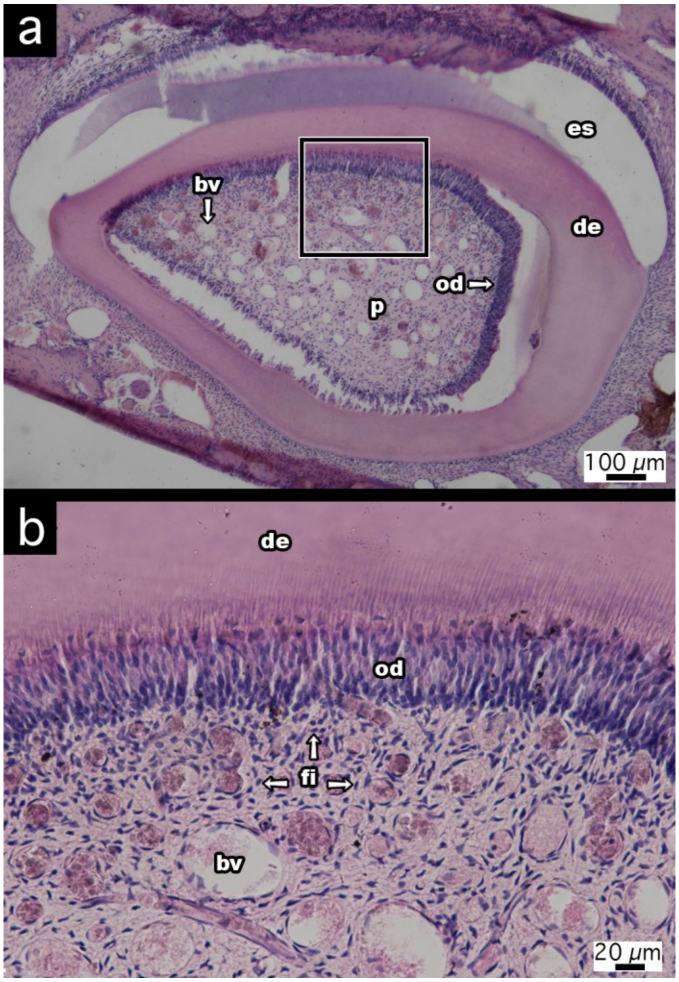
a
es
bv
de
od
p
100 μm
b
de
od
fi
bv
20 μm

3.3.2 Hard tissues of the hadrosaurid dentary tooth

The hadrosaurid tooth has a rounded or oval root in cross section and becomes more laterally compressed with distinct surfaces toward the tip (Figure 3.1b). Because the shape of the tooth changes along the apical-occlusal axis (Figure 3.1b), the thin section images will vary in shape depending on the height they were made in the tooth. Thin sections near the tip of a tooth will appear more pentagonal in shape, with the denticles and median carina of the enamel forming the three points, whereas thin sections from the root will be more rounded. In the maxillary teeth, enamel is on the labial face of the crown, and is present on most teeth in the occlusal surface (Figure 3.1c, e). In the dentary, the enamel is only seen on the lingual face of the youngest occluding tooth crown of each tooth family – in all other teeth, the enamel has been worn away during occlusion with the maxillary dental battery (Figure 3.1d, e). This enamel is turned into a cutting edge, and the exposed dentine of the other teeth serves as a grinding surface, a process similar to a rodent incisor (Osborn 1969, Shellis and Berkovitz 1981).

Under cross-polarized light three layers of enamel are visible (Figure 3.5a): (1) the inverted basal unit layer – sensu Sander (1999) – at the dentine-enamel junction (DEJ) with enamel spindles, (2) the coarse wavy enamel making up the bulk of the enamel and, (3) the thin outer layer of fine wavy enamel. The lines comprising the fine wavy enamel are not visible using a light microscope, but have been previously reported from SEM images (Sander 1997, 1999, Hwang 2005, 2011). The presence of wavy enamel is a synapomorphy of iguanodontids and hadrosaurs (Sander 1999, Hwang 2005). The enamel spindles in the basal layer are produced when odontoblasts that have extended into the ameloblast layer become trapped as enamel formation begins (Nanci 2013). These dark thin projections are visible throughout the DEJ (Figure 3.5b), as in other ornithischians (Wang et al. 2015).

The dentine directly underlying the cementum-covered portion of the hadrosaurid tooth is mantle dentine (Figure 3.5c). Erickson et al. (2012) reported mantle dentine as a thick layer in hadrosaurid teeth and played a crest-forming role in the lower dental batteries. However, this study reports mantle dentine as a thin layer along the CDJ that is on average 15 µm thick in the adult and 17 µm thick in the perinate. This layer lacks dentinal tubules, which is similar to mantle dentine in mammalian species (Goldberg et al. 2011). The mantle dentine is light coloured in plain polarized light and is highly birefringent under cross-polarized light. Separating the mantle dentine and the remaining primary dentine in some areas is a dark globular layer of dentine, called the granular layer of Tomes (Nanci 2013) (Figure 3.5c). Bordering the mantle dentine/granular layer of Tomes is a thick, whiter band of primary dentine (Figure 3.5c). This band of dentine contains dentinal tubules and has an average thickness of 170 µm along the cemento-dentine junction (CDJ) of the adult and 105 µm in the perinate.

A darker dentine comprises the remaining primary dentine, and the dentinal tubules are continuous with those of the whiter band of dentine. In the adult specimen, this darker primary dentine has many elliptical intrusions, previously identified as transverse giant tubules by Erickson et al. (2012), giving this dentine a disorganized appearance (Figure 3.5d). The dentine around these intrusions is atubular, sclerotic, and lighter in colour. The pulpward migration of the odontoblasts either stops at, or is redirected around these intrusions. Another irregularity seen in the darker primary dentine is where odontoblasts appear to converge with odontoblasts from the opposite side of the tooth (Figure 3.5e). The odontoblasts either halt when they converge, or form pockets as seen from the spaces within the dentine (Figure 3.5e). These pockets, previously identified as longitudinal giant tubules by Erickson et al. (2012), likely contained trapped pulp with blood vessels and fibroblasts.

In the perinatal specimen, the primary dentine is less complex and lacks the elliptical intrusions (Figure 3.5f), a difference first noted by Erickson and Zelenitsky (2014). The perinatal teeth show thin concentric rings throughout the dentine, which have been called lines of von Ebner (Erickson 1996). These concentric rings look similar those in the primary dentine of other extant and fossil species (Rosenberg and Simmons 1980, Erickson et al. 2015, García and Zurriaguz 2015, Fong et al. 2016). The colour of the dentine in the perinate is consistent throughout the tooth and darkens slightly towards the pulp cavity, which may be a result of an increased density of dentinal tubules (Fosse et al. 1992, Mjör and Nordahl 1996).

In the dentine underlying the enamel of the hadrosaurid tooth, the dentine adjacent to the enamel appears to be a more diffused variation of the thick, whiter band of primary dentine seen along the opposite face of the tooth (Figure 3.5g, h). This layer of dentine below the DEJ merges with the whiter band of the cementum-associated dentine (Figure 3.5h). The boundary between this lighter band under the DEJ and the darker primary dentine is irregular (Figure 3.5g).

3.4 Discussion

A problem in paleontology is the rarity of preserved soft tissues. Soft tissues help explain many biological processes (Witmer 1995), which is why it is necessary to reconstruct them using extant analogues. As the soft tissues (pulp vasculature and cells) are not preserved in hadrosaurid teeth, reconstruction of dentinogenesis requires the use of a living analogue. This analogue must exhibit a detailed similarity of gross anatomy as well as histological structure and organization that imply a similar method of development. Initial comparisons with the complex grinding teeth of modern horses and bison provide little information on the formation of the hard tissues of the hadrosaurid tooth, because the former consists of a series of complex tissue infoldings and overlaps, whereas

Figure 3. 5. Histology of the hadrosaurid tooth (UALVP 56336). **a**, cross-polarized image of enamel; **b**, magnified plain-polarized image of (**a**) showing enamel spindles; **c**, the cemento-dentine junction; **d**, image of the primary dentine; **e**, converging dentine, with evidence of odontoblasts having been diverted from their original course upon contacting odontoblasts from the opposite side; **f**, concentric rings of the perinate dentine; **g**, the more diffused dentine band at the dentine-enamel junction; **h**, image showing the diffused band of dentine at the dentine-enamel junction narrowing to a more prominent band under the cemento-dentine junction. All images are in transverse view; lingual is to the top in all images except (**h**); lingual is to the left in (**h**). Abbreviations: ac, acellular cementum; cc, cellular cementum; de, dentine; det, dentinal tubule; en, enamel; es, enamel spindles; glt, granular layer of Tome's; md, mantle dentine; pc, pulp cavity; wen, wavy enamel.

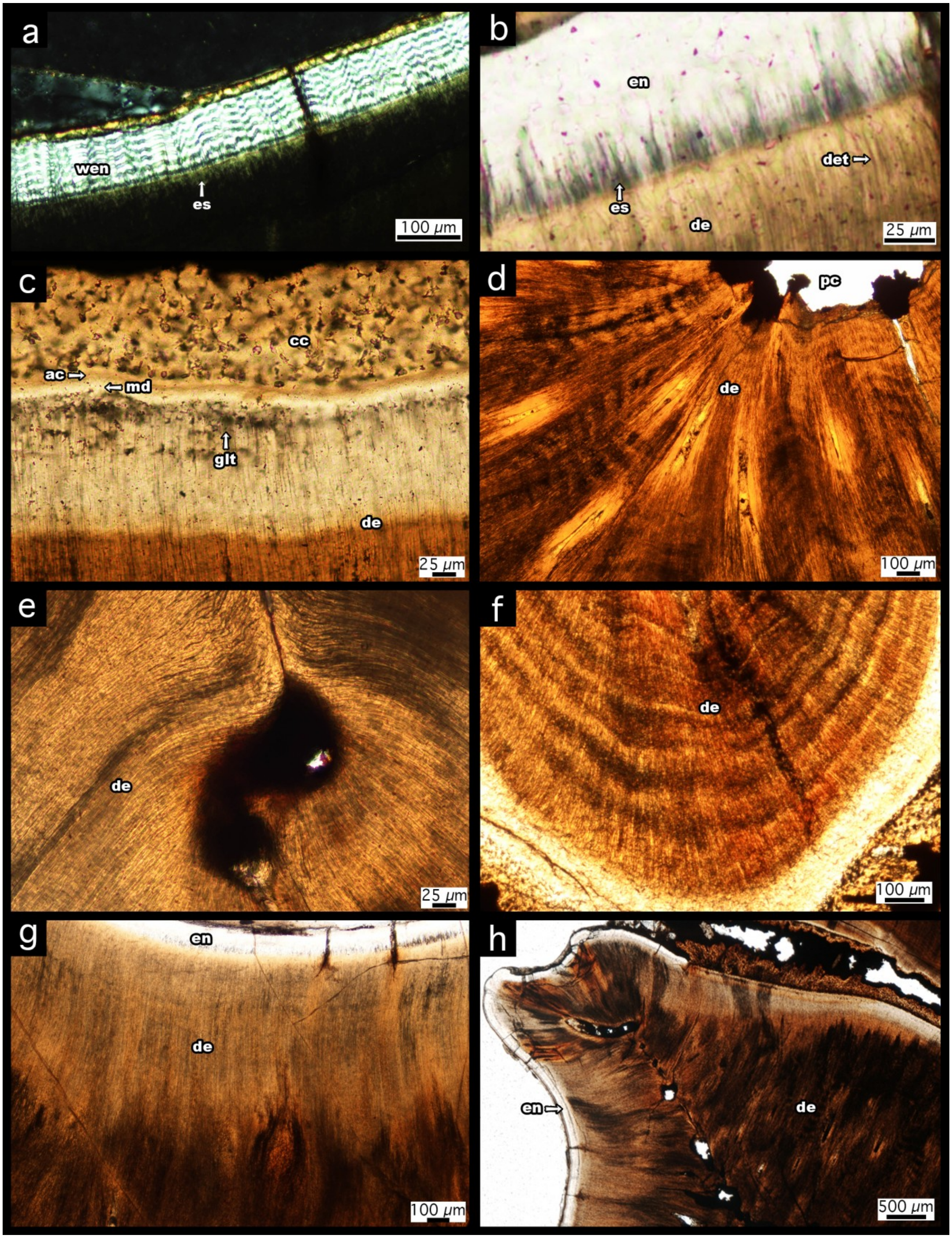
a
wen
es
100 μm
b
en
det
es
de
25 μm
c
cc
ac
md
glt
de
25 μm
d
pc
de
100 μm
e
de
25 μm
f
de
100 μm
g
en
de
100 μm
h
en
de
500 μm

the latter is actually much simpler in its overall construction. The hadrosaurid tooth most closely resembles rodent and lagomorph incisors in that the CEJ has shifted so that enamel covers only one side of the tooth rather than forming a cap. Because of this arrangement of hard tissues, the wear of the softer dentine and cementum layers leave a raised enamel cutting edge (LeBlanc et al. 2016b) (Figures 3.1b, 3.2a). However, the similarities extend beyond the arrangements of the crown and root tissues.

Mammalian ever-growing incisors have infilled pulp cavities at the occlusal end as a way of preventing a breached pulp cavity (Shellis and Berkovitz 1981, Ohshima and Yoshida 1992, Ali and Mubarak 2012) (Figure 3.6). Dentinogenesis in the incisors of modern rodents begins as the odontoblasts start depositing dentine while bordering the DEJ and CDJ (Figures 3.4, 3.7a, d). Next, the odontoblasts move towards the centre of the pulp, with some becoming blocked by the blood vessels supplying the pulp (Figure 3.7b, e). Here, the odontoblasts leave an undulating boundary in ground thin sections (Figure 3.2h). The vasculature of the pulp in the pika implicates blood vessels as the cause of this undulating dentine border. Finally, the odontoblasts progress to the centre of the pulp, leaving behind a tooth that is now filled with dentine (Figure 3.7c, f). The daily variation in deposition of dentine creates lines of von Ebner in the beaver (Rinaldi and Cole 2004) (Figure 3.2g).

Using the mammalian ever-growing incisor as a model, the process of dentinogenesis may be inferred for the hadrosaurid tooth. In the perinatal hadrosaurid, odontoblasts appear to begin depositing dentine from the DEJ and CDJ (Figure 3.7a, g), and continue towards the centre of the pulp, as in modern rodents. The perinatal hadrosaurid tooth has an undulating dentine border in thin section (Figure 3.7b, h), similar to the undulating border seen in the beaver (Figure 3.2h). As the odontoblasts move toward the centre of the pulp, the tooth is filled in with dentine

(Figure 3.7c, i). Concentric rings in the dentine potentially represent the daily deposition of dentine (lines of von Ebner), as they do in the beaver incisor (Rinaldi and Cole 2004).

In the adult hadrosaurid, dentinogenesis likely would have begun the same way, with the odontoblasts lining the DEJ and CDJ and moving towards the centre of the pulp (Figure 3.8a). As the odontoblasts move through the pulp, elliptical intrusions are left behind; an undulating border of dentine is also visible (Figure 3.8b, d, e). When the odontoblasts reach the centre of the pulp, the tooth is filled with dentine, but with many of these elliptical intrusions interrupting the lines of von Ebner (Figure 3.8c, f).

A variation in dentinogenesis from the extant analogues is found in the proximal tips of the hadrosaurid teeth. This area of the tooth is more pentagonal in shape in hadrosaurids, suggesting that the movement of the odontoblasts was different than in the rounded base of the tooth. The odontoblasts again began secreting dentine from the DEJ and CDJ (Figure 3.8g) and moved towards the centre of the pulp. However, due to the shape of this part of the tooth, many odontoblasts would have converged with their counterparts before reaching the centre of the pulp (Figure 3.8h, k), creating pockets of the former pulp cavity (Figure 3.8j). This continued until the odontoblasts reach the centre of the pulp (Figure 3.8i, l).

The modern rodent incisors and the perinatal hadrosaurid teeth appear to have similar processes of dentinogenesis, resulting in the pulp cavities replaced by dentine with the concentric rings of von Ebner lines (Figure 3.7f, i). This is not the case for the adult hadrosaurid (Figure 3.8f). The concentric rings of dentine, which are unmistakable in the perinate, are interrupted by many elliptical intrusions in the adult thin sections, which are referred to as transverse giant tubules by Erickson et al. (2012) and Erickson and Zelenitsky (2014) and as blood vessels by (LeBlanc et al. 2016b). Using the mammalian ever-growing incisor as a model for the vascularity of pulp cavities (Figure 3.4), these elliptical intrusions are identified as blood vessels, which is in

Figure 3. 6. Comparisons between the hard tissues of the hadrosaurid tooth and mammalian ever-growing incisor. **a**, ROM 3500, coronal view of hadrosaurid tooth; **b**, UALVP 56918, sagittal view of rabbit incisor (*Oryctolagus cuniculus*; UALVP 56918). Abbreviations: ce, cementum; cej, cemento-enamel junction; de, dentine; en, enamel, pc, pulp cavity. Image of ROM 3500 taken by A. LeBlanc, used with permission.

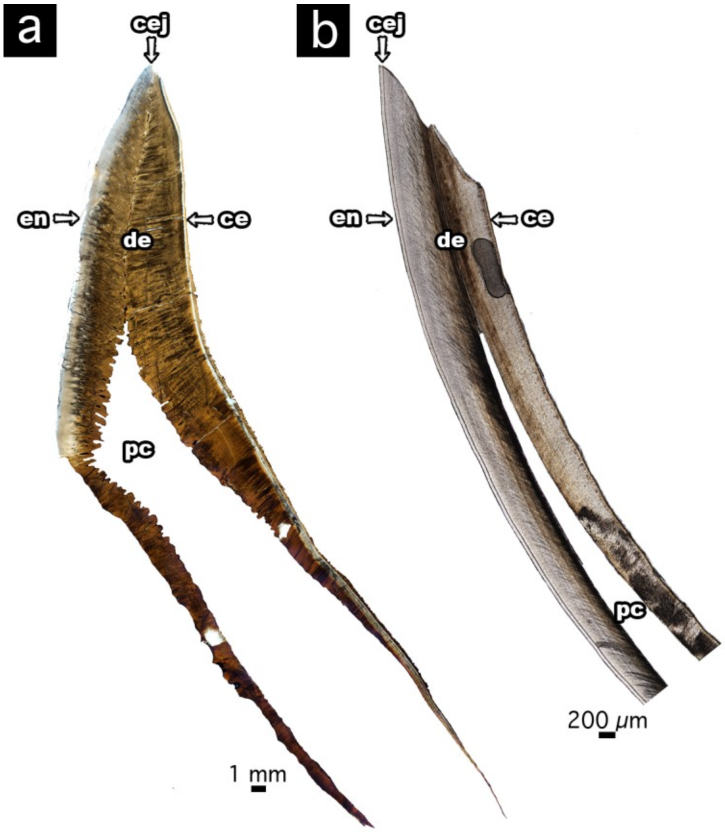
a
cej
en
de
ce
pc
1 mm
b
cej
en
de
ce
pc
200 μm

Figure 3. 7. Dentinogenesis in the mammalian ever-growing incisor and perinatal hadrosaurid tooth. **a**, stage 1, the odontoblasts start dentinogenesis lining the dentine-enamel junction and cemento-dentine junction; **b**, stage 2, the odontoblasts move towards the centre of the pulp, with some becoming blocked by blood vessels; **c**, stage 3, the odontoblasts progress to the centre of the pulp, creating a tooth that is now filled with dentine. **d-f**, stages 1 to 3 of the beaver incisor (*Castor canadensis*, UALVP 56917); **g-i**, stages 1-3 of the perinatal hadrosaurid tooth (UALVP 54419). All scale bars are 500 µm. Abbreviations: bv, blood vessel.

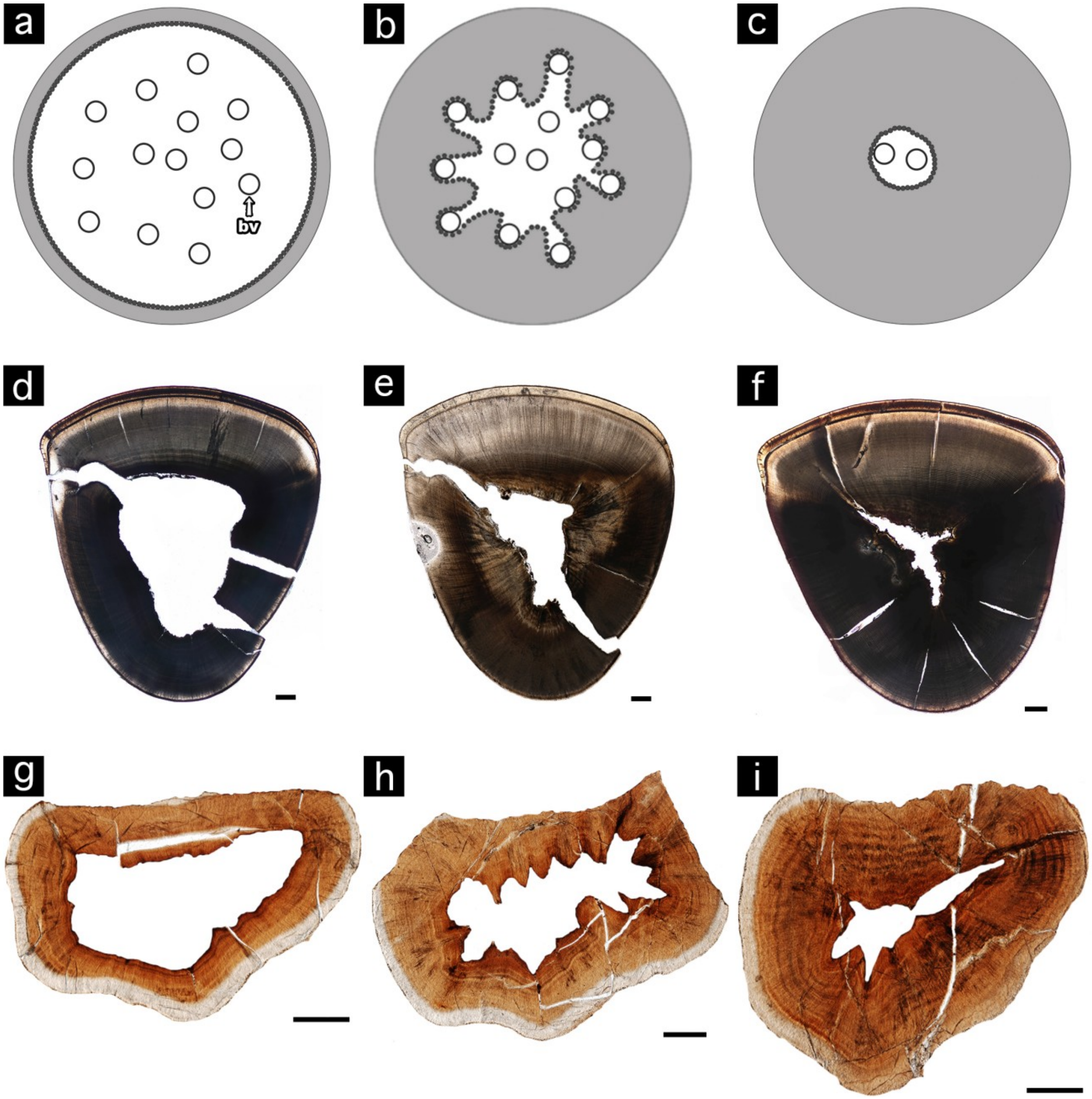

a
b
c
bv
d
e
f
g
h
i

Figure 3. 8. Modified dentinogenesis of the adult hadrosaurid tooth (UALVP 56336) and the tip of the hadrosaurid tooth. **a**, stage 1, the odontoblasts start dentinogenesis lining the dentine-enamel junction and cemento-dentine junction; **b**, stage 2, the odontoblasts move towards the centre of the pulp, with some becoming blocked by blood vessels; **c**, stage 3, the odontoblasts progress to the centre of the pulp, creating a tooth that is now filled with dentine. The rapidly growing dentine in (**b**) and (**c**) entombed the blood vessels of the pulp before they had the ability to recede. Entombed blood vessels were left in the wake of the odontoblasts. **d**, magnified image of the vascular spaces within the dentine, white arrows indicate the vascular spaces (that the blood vessels previously occupied); **e-f**, stages 2-3 of the adult hadrosaurid; **g**, stage 1of dentinogenesis in the tip of the hadrosaurid tooth, the odontoblasts start dentinogenesis lining the dentine-enamel junction and cemento-dentine junction; **h**, stage 2, the odontoblasts move towards the centre of the pulp, with some converging with odontoblasts from the opposite side of the tooth, creating pockets of pulp; **i**, stage 3, the odontoblasts progress to the centre of the pulp, creating a tooth that is now filled with dentine with multiple pockets of pulp, **j**, magnified image of the pocketing of the pulp cavity, white arrows indicating pockets of pulp; **k-l**, stages 2-3 of dentinogenesis in the tip of the hadrosaurid tooth. Abbreviations: bv, blood vessel; pcp, pulp cavity pocket; vs, vascular space.

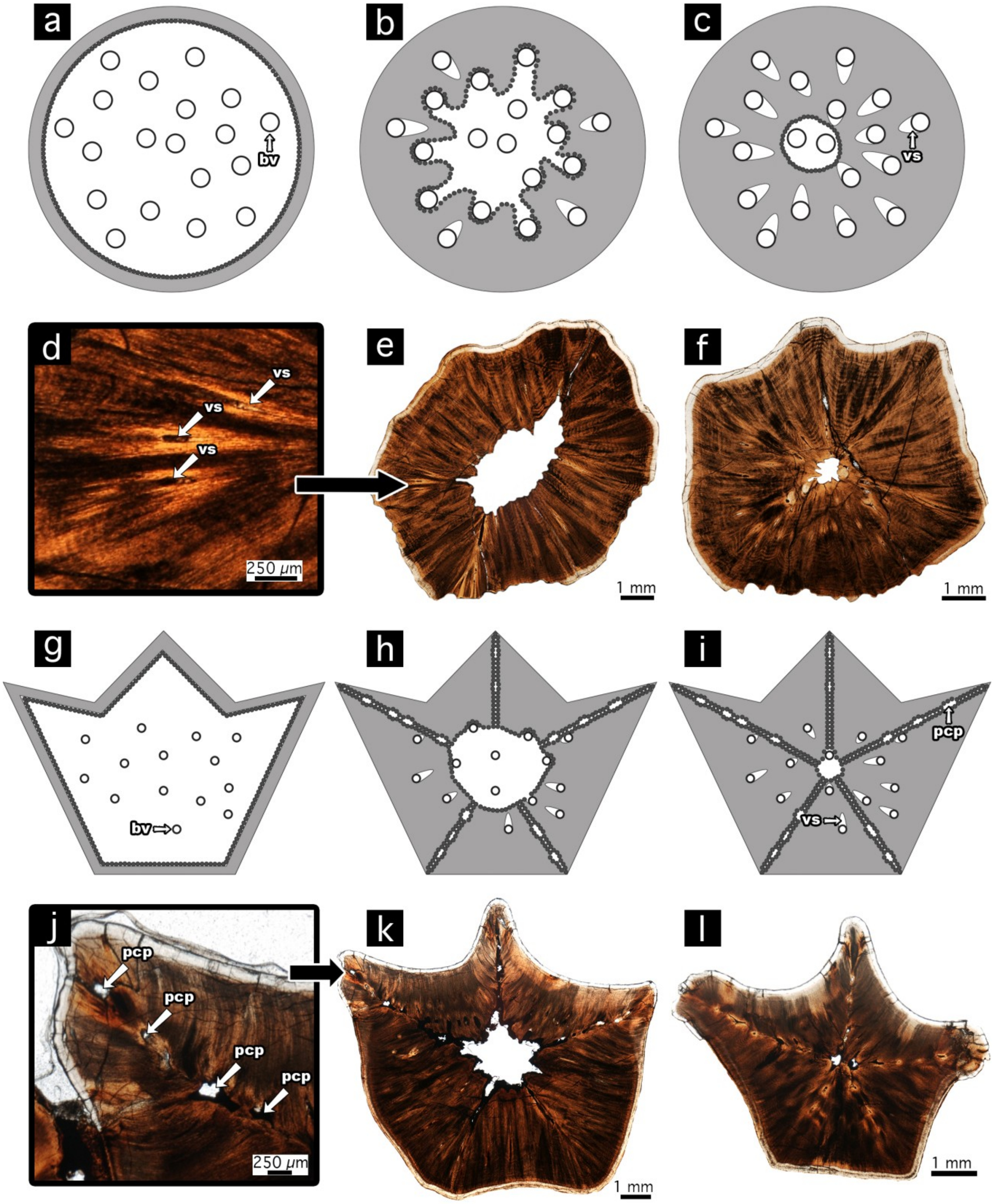
a
bv
b
c
vs
d
vs
vs
vs
250 μm
e
1 mm
f
1 mm
g
bv
h
i
pcp
vs
j
pcp
pcp
pcp
pcp
250 μm
k
1 mm
l
1 mm

agreement with the interpretations of LeBlanc et al. (2016). The advancing dentine entombed the blood vessels of the pulp before they had the ability to recede, which then closed off and secreted atubular sclerotic dentine around the former blood vessels (Figures 3.5d; 3.8d). As the odontoblasts advanced toward the centre of the pulp, many entombed blood vessels were left in their wake. This trapping of blood vessels may have been a result of a change in the rate of tissue development (heterochrony), in that dentinogenesis was accelerated in adult teeth, or alternatively, the recession of the pulp cavities proceeded at a slower rate than in the perinate. The perinatal specimen had six tooth families with only one replacement tooth underneath each functional tooth that was in occlusion (Appendix 3.1, Figure A-3.3). The adult specimen, on the other hand, had 40 tooth families with three to four replacement teeth below each functional tooth (Appendix 3.1, Figure A-3.4). This acceleration in dentinogenesis may have been a product of the adult hadrosaurid needing to develop and replace far more teeth than the perinate did. Exploring this change in the rate of tissue development within the hadrosaurid tooth may assist in better understanding ontogeny of the dental battery.

Looking at hadrosaurid teeth from a developmental perspective, and using the mammalian ever-growing incisor as an extant analogue, provides context for structures observed in histological section. Erickson et al. (2012) used the terms transverse and longitudinal giant tubules to describe infilled branches of the pulp cavity. However, this study suggests that the transverse giant tubules are actually entombed blood vessels (Figure 3.8d) and the longitudinal giant tubules are remnants of the pulp cavity (Figure 3.8j), providing a dual origin for the “giant tubules” identified by these authors.

Although the crest-forming abilities of the American bison and horse teeth make them an appealing extant analogue for hadrosaurid teeth, these ungulates have a different approach for resisting an abrasive diet. Rather than constantly replacing worn teeth, like the hadrosaurid dental battery, the bison and horse have hypsodont (high crowned) dentition (Damuth and Janis 2011). These differences in tooth wear strategies lead to different requirements of the dental tissues. There is greater complexity in the formation of the crests and dental tissues of ungulate grinding teeth, with coronal cementum enveloping the entire tooth crown at eruption (Listgarten 1968, LeBlanc et al. 2016b). On the other hand, the cutting surfaces of the hadrosaurid tooth and mammalian ever-growing incisor only required a shift of the CEJ and an evolutionary increase in the rate of dentinogenesis (LeBlanc et al. 2016b). This makes the mammalian ever-growing incisor a more useful extant analogue. This incisor and the hadrosaurid tooth use the same hard tissue arrangement and continuous eruption as the strategy for processing a highly abrasive diet.

3.4.1 Crestal dentine – a new type of dentine?

The ground thin sections of beaver and rabbit incisors reveal a band of primary dentine adjacent to the enamel (Figure 3.2e, f). This banding may be a result of changes in the orientations of collagen fibers or calcospherites compared to the remainder of the dentine (Shellis 1981). A band of primary dentine is also seen in each hadrosaurid tooth (Figure 3.5c), but it seems to have little in common with the primary dentine of the mammalian incisor. In the hadrosaurid, this band is located along the cementum covered portion of the tooth (i.e., on the opposite side of the tooth relative to its position in the rodents and lagomorphs) and appears to play a structural role by forming a crest along the cementum-related portion of the tooth. These crests act as secondary wear surfaces, whereas the enamel is the primary wear surface (Figure 3.1d). Given the lack of any known comparable dental tissue in extant or extinct vertebrates, a new dentine type is being proposed.

Etymology: Named for the crests on the occlusal surface of worn hadrosaurid teeth that are formed by this dentine band.

Characterization: Crestal dentine is described as a new subtype of primary dentine. Crestal dentine is located primarily along the CDJ in dentary and maxillary teeth and forms secondary ridges throughout the occlusal surface of a tooth family in the dentary, creating basins within the occlusal surface of the dentary dental battery as the softer layers of dentine are quicker to wear away (Figure 3.1d). These secondary wear surfaces are absent in the maxilla, because the crests are formed entirely by the labial-facing enamel of the maxillary dental battery (Figure 3.1c).

Crestal dentine has been previously identified as mantle dentine (Erickson et al. 2012, Erickson and Zelenitsky 2014, Mallon and Anderson 2014); however mantle dentine is too thin to be seen without a microscope as it is typically 15-30 µm in mammals (Goldberg et al. 2011, Nanci 2013). Crestal dentine is easily visible without the use of a microscope and is an order of magnitude thicker than mantle dentine (Figure 3.1d). Crestal dentine also has dentinal tubules, whereas mantle dentine generally does not (Goldberg et al. 2011) (Figures 3.5c, 3.9c). A thin atubular mantle dentine is seen between the acellular cementum and crestal dentine at the CDJ of the hadrosaurid tooth (Figure 3.5c), but is not seen along the DEJ (Figure 3.5g). Furthermore, previous studies (Wang et al. 2015, Brink et al. 2016) have shown mantle dentine to be absent along the DEJ in hadrosaurid dinosaurs or other ornithischians, as the dentinal tubules of the primary dentine abut and sometimes extend into the enamel as enamel spindles. However, these authors (Wang et al. 2015, Brink et al. 2016) showed that mantle dentine occurs along the DEJ in saurischians.

Under plain polarized light, crestal dentine is whiter in thin section compared to the remaining primary dentine, and is seen in every tooth of both perinatal and adult hadrosaurid dentaries (Figure 3.9a, b, d). This likely represents hypercalcification or some other chemical difference between crestal dentine and the remaining dentine types. The dentine tubules are continuous across the crestal and more internal dentine layers, but under cross-polarized light, the crestal dentine appears birefringent (Figure 3.9c), likely due to the organization of the crystalline matrix. The expanded crestal dentine below the DEJ merges with the more salient band of the cementum-associated dentine (Figure 3.9e). This layer of dentine also has a higher density of dentinal tubules at the DEJ (Brink et al. 2016) and CDJ, with some extending across the DEJ into the enamel as enamel spindles (Figure 3.5b). This increased density of dentinal tubules along the DEJ increases the hardness of the crestal dentine (Brink et al. 2016), potentially in conjunction with a hypercalcified surrounding matrix. Regardless of the mechanism, the increased hardness of this dentine layer forms the crests of the tessellated pavement pattern along the hadrosaurid dental battery. Erickson et al. (2012) confirm the crest forming abilities of crestal dentine, although they refer to it as mantle dentine.

The whiter colour of crestal dentine in plain polarized light in both the adult and perinate specimens (Figure 3.5c, f) suggests that it has a different chemical structure than the other types of dentine. This white colouration must represent a biochemical or crystalline structure that reacts differently during fossilization than the other dentine types. Conversely, the crestal dentine may be whiter coloured in plain polarized light and birefringent in cross-polarized light because it is translucent like enamel. This may be the result of the presence of a glassy intertubular matrix, like that in sclerotic dentine. The dentine may be hypercalcified early in dentinogenesis before transforming into the typical calcification process.

Crestal dentine could compensate for the lack of enamel in the older tooth generations of each tooth family in the dentary. In the maxilla, enamel is on the labial face of the tooth (Lull and Wright 1942) and the enamel is not resorbed or worn away as new teeth are added to the tooth family (Figure 3.1c, e). Crestal dentine in the dentary could be acting as the enamel seen in the maxilla, creating secondary grinding surfaces within each tooth family (Figure 3.1d, e). Although

Figure 3. 9. Crestal dentine in the adult hadrosaurid (UALVP 56336). **a**, a whole tooth showing the crestal dentine; **b**, magnified image of box labeled b in (**a**) in plain polarized light; **c**, magnified image of box labeled b in (**a**) in cross-polarized light; **d**, magnified image of box labeled d in (**a**), crestal dentine under the dentine-enamel junction; **e**, crestal dentine under the dentine-enamel junction merging with the crestal dentine associated with the cementum. Abbreviations: ac, acellular cementum; cc, cellular cementum; cd, crestal dentine; de, remaining primary dentine; md, mantle dentine; pc, pulp cavity.

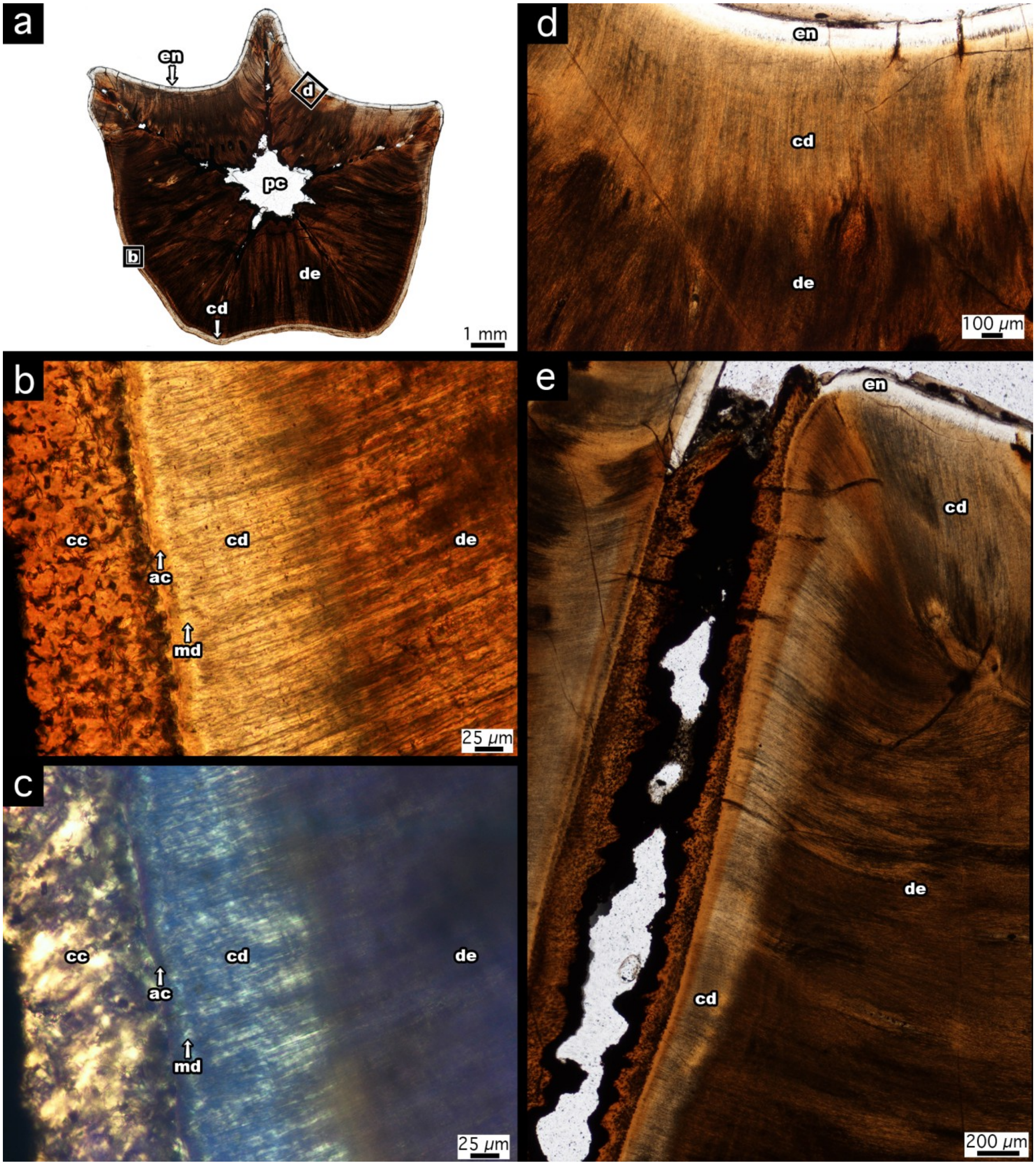
a
en
d
pc
b
de
cd
1 mm
d
en
cd
de
100 μm
b
cc
cd
de
ac
md
25 μm
c
cc
cd
de
ac
md
25 μm
e
en
cd
de
cd
200 μm

the teeth in the maxilla also have crestal dentine, it does not serve the function of creating multiple crests. It is possible that its presence in the teeth of the maxillary battery is simply an indirect consequence of a common development process shared with the teeth of dentary, where the crestal dentine is essential for forming the shearing surface. Future research on the phylogenetic distribution of this tissue can help understand its evolutionary significance.

3.5 Conclusions

Histological analysis of the mammalian ever-growing incisor reveals that it is an excellent model for understanding dentinogenesis in hadrosaurid teeth. The constant wear, eruption, and hard tissue formation in the ever-growing incisor match very well with the same phenomena in individual hadrosaurid teeth. Using this model to explore dentinogenesis within the hadrosaurid tooth provides a developmental context to histologic structures identified in previous studies. Dentinogenesis in the perinatal hadrosaurid tooth is extremely similar to that of the rodent incisor, and comparisons with that of the adult hadrosaurid tooth reveal a possible heterochronic shift in the rates of dentinogenesis and pulp recession, creating the complex structures found within the dentine of adult hadrosaurid teeth. The transverse and longitudinal giant tubules of previous studies (Erickson et al. 2012, Erickson and Zelenitsky 2014) were probably the result of odontoblasts enveloping blood vessels or converging on each other to form pockets of the remaining pulp during dentinogenesis. Using these extant analogues as a way to reconstruct the soft tissues of the hadrosaurid tooth helps fill in the gaps of knowledge regarding these unique teeth. This study also revealed a new tissue in hadrosaurids, crestal dentine. As a result of its chemical composition and tubular structure, is harder than regular dentine, allowing it to functionally replace enamel in the teeth of the lower dental battery to form the lower half of the shearing surface.

Appendix 3.1

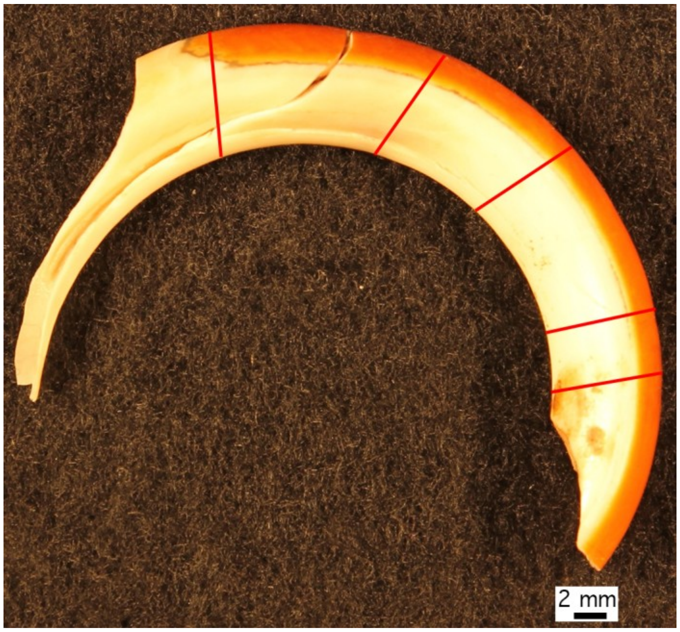

Figure A-3. 1. Cuts made of the beaver incisor (*Castor canadensis*; UALVP 56917).

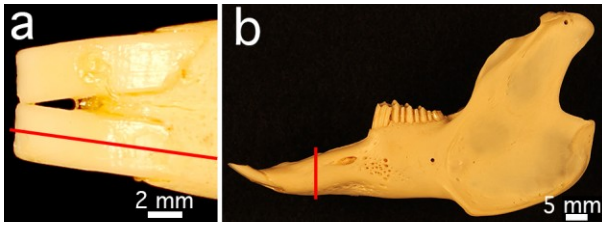

Figure A-3. 2. Cuts made of the rabbit incisor (*Oryctolagus cuniculus*; 56918). **A**, occlusal view; **B**, cut made to detach incisors from jaw.

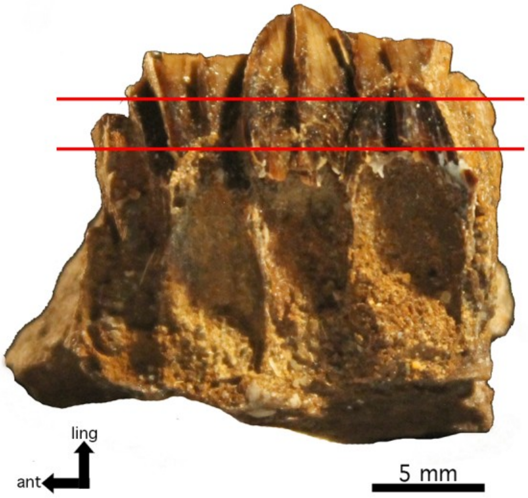

Figure A-3. 3. Cuts made of the perinatal hadrosaurid dental battery (UALVP 54419)

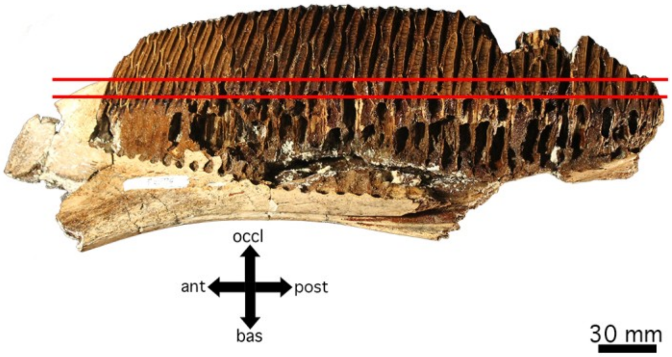

Figure A-3. 4. Cuts made of the adult hadrosaurid dental battery (UALVP 56336)

Chapter 4: Conclusion

In this thesis, the first histological thin sections of an entire hadrosaurid dentary dental battery are presented. These transverse thin sections provided information on the soft and hard tissue interactions inside the dental battery, and demonstrate the ontogenetic changes in the interactions that occurred between perinatal and adult stages. The periodontal ligaments (PDL) connected the teeth to each other, as well as to the alveolar bone, throughout the entire dental battery. The extent of PDL attachments was previously suspected in some studies but unknown. The transverse thin sections of the PDL added to a previous study showing a PDL connection within the tooth family in coronal view (LeBlanc et al. 2016b). These ligamentous connections allowed for tooth migration within the dental battery. Signs of migration included alveolar bone remodeling, the angle of alveolar septa when compared to the longitudinal axis of the dentary, the anterior orientation of newer tooth generations within a single tooth family, and the extensive resorption seen in the most anterior tooth families of the dental battery. Before this study, the extent of tooth migration within the dental battery was unknown.

In the specimen of the perinatal hadrosaur, the shift was only anterior, whereas in the adult most of the dental battery shows migration towards the front, whereas the most posterior tooth families are directed posteriorly. These differences suggest tooth migration begins early in ontogeny, as all alveolar septa are anteriorly oriented in the perinate. However, it is possible that alveoli were added to the back of the dental battery. A posterior shift is only seen in the thin sections of the adult specimen. This may be a product of occlusal forces acting upon a dental battery that was no longer adding tooth families. The transverse histological thin sections of an entire hadrosaurid dentary dental battery illustrate the dynamic movement within the dental battery. This provides substantial evidence that the dental battery is not as solid as previously thought (Cope 1883, Ostrom 1961, Erickson et al. 2012, Erickson and Zelenitsky 2014) as the teeth are not cemented together. This also explains why hadrosaurid jaws are often found without teeth in the alveoli, and why unworn and unerupted hadrosaur teeth are also found as isolated specimens in places like Dinosaur Provincial Park.

Histological thin sections of the ever-growing incisors of an extant beaver (Castor *canadensis*), rabbit (*Oryctolagus cuniculus*), and pika (*Ochotona* sp.) revealed numerous similarities with hadrosaurid teeth. These similarities include; (1) the shift of the cemento-enamel junction (CEJ); (2) the cutting-edge occlusal surface that is a result of the shift in the CEJ and the wear of the softer dentine and cementum; (3) the periodontal ligamentous attachment seen on the side of the tooth covered by cementum, (4) the lack of any ligamentous attachments on the side of the tooth covered with enamel; (5) continuous tooth eruption (the continuous tooth replacement within a tooth family is functionally similar to the continuous eruption of the ever-growing incisor); (6) the need to plug the pulp cavity with dentine at the occlusal end in order to prevent a breached pulp cavity on the occlusal surface; and, (7) similarities in dentine growth, as the pulp cavity is plugged in a zipper-like process, beginning at the distal tip. For these reasons, and building on the work of LeBlanc et al. (2016), the mammalian ever-growing incisor has been proposed as an extant analogue for the hadrosaurid tooth family. The mammalian ever-growing incisor has a stronger resemblance – physically and developmentally – to a hadrosaur tooth family than the ever-growing teeth of American bison and horse that are the commonly used extant analogues.

Using the ever-growing incisor as an analogue, hypotheses for dentinogenesis in the hadrosaurid tooth were developed. The pulp seen in the pika thin sections, which is a tissue that is not preserved in hadrosaurid teeth, gave an indication of how vascular the pulp may have been in hadrosaurids. As the odontoblasts move towards the centre of the pulp in the ever-growing incisor (and presumably in a tooth of the perinatal hadrosaurid), they stop at or divert around the blood vessels. The blood vessels then recede, leaving the concentric rings of the lines of von Ebner uninterrupted. For the adult hadrosaurid, there is a difference in dentinogenesis. Either the odontoblasts were moving faster, or the blood vessels of the pulp were receding more slowly, and the blood vessels became entombed within the dentine, creating elliptical intrusions that interrupt the concentric rings of the dentine. These entombed blood vessels were termed “transverse giant tubules” by Erickson et al. (2012). The tip of the hadrosaurid tooth also has a different pattern of dentinogenesis. As the tip is more pentagonal in shape, most of the odontoblasts do not reach the centre of the pulp cavity. Rather, in the regions of the “corners” of the pentagon, they converge with the odontoblasts from the opposite side and create pockets of pulp. This pocketing was termed “longitudinal giant tubules” by Erickson et al. (2012). The variation in dentinogenesis between the perinate and adult specimens may be a result of the increased number of teeth in the adult hadrosaurid, and the need to develop over 300 teeth per dentary. The perinate had only six tooth families in the dentary dental battery with one successional tooth per family, whereas the adult specimen had 40 tooth families with approximately three to four successional teeth per family. This increase in the numbers of teeth may have resulted in the need for faster dentinogenesis.

Finally, in this thesis a new subtype of primary dentine is proposed for the hadrosaurid tooth. Crestal dentine appears as a thick band along the cementum-related region of the tooth. It is wider and more diffuse than in the part of the tooth associated with enamel. It is white in plain polarized light and birefringent under cross-polarization. This dentine was previously identified as mantle dentine (Erickson et al. 2012, Erickson and Zelenitsky 2014, Mallon and Anderson 2014), even though mantle dentine is typically atubular, 15-30 µm thick in mammals, and is invisible to the naked eye. Crestal dentine, on the other hand, is tubular, has tubules that are continuous with those of the remaining primary dentine, and is thick enough to be seen without a microscope. This sublayer of dentine is harder than the regular primary dentine based on chemical composition and tubular structure. This has also been established by Erickson et al. (2012), although the authors refer to it as mantle dentine. The increased hardness of crestal dentine creates basins within the wear surface of a hadrosaurid tooth, as the softer remaining primary dentine is quicker to be is worn away. This crest-forming feature allows it to create secondary wear surfaces throughout the occlusal surface.

The transverse histological thin sections of the perinatal and adult hadrosaurid dentary dental batteries have provided information on the ontogeny, growth, dynamics, and hard tissue development within the dental battery. Future research should focus on doing the same kind of studies on subadult hadrosaurid jaws that were still growing at the time of death in order to refine the timing of when the ontogenetic changes occurred within the dental battery, and to learn more details about how alveoli are added to the dental battery.

Literature Cited

Ali, Z.H., and Mubarak, R. 2012. Histomorphological study of dentine pulp complex of continuously growing teeth in the rabbits. Life Science Journal, **9**: 1554–1564.

Beertsen, W. 1975. Migration of fibroblasts in the periodontal ligament of the mouse incisor as revealed by autoradiography. Archives of Oral Biology, **20**: 659–666. doi:10.1016/0003-9969(75)90134-X.

Beertsen, W., Everts, V., and van den Hooff, A. 1974. Fine structure of fibroblasts in the periodontal ligament of the rat incisor and their possible role in tooth eruption. Archives of Oral Biology, **19**: 1087–1098. doi:10.1016/0003-9969(74)90235-0.

Beertsen, W., and Hoeben, K.A. 1987. Movement of fibroblasts in the periodontal ligament of the mouse incisor is related to eruption. Journal of Dental Research, **66**: 1006–1010. doi:10.1177/00220345870660050201.

Bell, P.R., Fanti, F., Currie, P.J., and Arbour, V.M. 2014. A mummified duck-billed dinosaur with a soft-tissue cock's comb. Current Biology, **24**: 70–75. Elsevier Ltd. doi:10.1016/j.cub.2013.11.008.

Berkovitz, B.K.B. 1981. Tooth eruption. *In* Dental anatomy and embryology. *Edited by* J.W. Osborn. Blackwell Scientific Publications, Oxford. pp. 309–318. Available from http://onlinelibrary.wiley.com/doi/10.1002/cbdv.200490137/abstract%5Cnhttp://onlinelibrary.wiley.com/doi/10.1525/ae.1985.12.2.02a00020/abstract%5Cnhttp://doi.wiley.com/10.1525/aa.2005.107.1.019%5Cnhttp://books.google.com/books?hl=en&lr=&id=_qPSLy9564cC&oi.

Brett-Surman, M.K. 1979. Phylogeny and palaeobiogeography of hadrosaurian dinosaurs. Nature, **277**: 560–562. doi:10.1038/277560a0.

Brett-Surman, M.K., and Wagner, J.R. 2007. Discussion of character analysis of the appendicular anatomy in Campanian and Maastrichtian North American hadrosaurids - variation and ontogeny. *In* Horns and Beaks: ceratopsian and ornithopod dinosaurs. *Edited by* K. Carpenter. Indiana University Press, Bloomington. pp. 135–169.

Brink, K.S., Chen, Y.-C., Wu, Y.-N., Liu, W.-M., Shieh, D.-B., Huang, T.D., Sun, C.-K., and Reisz, R.R. 2016. Dietary adaptions in the ultrastructure of dinosaur dentine. J. R. Soc. Interface, **13**: 20160626. doi:10.1098/rsif.2016.0626.

Brink, K.S., Zelenitsky, D.K., Evans, D.C., Horner, J.R., and Therrien, F. 2014. Cranial morphology and variation in *Hypacrosaurus stebingeri* (Ornithischia: Hadrosauridae). *In* Hadrosaurs. *Edited by* D.A. Eberth and D.C. Evans. Indiana University Press, Bloomington. pp. 245–265.

Brown, B. 1914. *Corythosaurus casuarius*, a new crested dinosaur from the Belly River Cretaceous, with provisional cloassification of the family Trachodontidae. Bulletin of the American Museum of Natural History, **33**: 559–565.

Budney, L.A. 2004. A survey of tooth attachment histology in Squamata: The evaluation of tooth attachment classifications and characters. University of Alberta.

Budney, L.A., Caldwell, M.W., and Albino, A. 2006. Tooth socket histology in the Cretaceous snake *Dinilysia*, with a review of amniote dental attachment tissues. Journal of Vertebrate Paleontology, **26**: 138–145. doi:10.1671/0272-4634(2006)26[138:TSHITC]2.0.CO;2.

Caldwell, M.W., Budney, L.A., and Lamoureux, D.O. 2003. Histology of tooth attachment tissues in the Late Cretaceous mosasaurid *Platecarpus*. Journal of Vertebrate Paleontology, **23**: 622–630. doi:10.1671/0272-4634(2003)023.

Chin, K. 2007. The paleobiological implications of herbivorous dinosaur coprolites from the Upper Cretaceous Two Medicine Formation of Montana: why eat wood ? Society for

Sedimentary Geology, **22**: 554–566. doi:10.2110/palo.2006.p06-087r.

Cope, E.E. 1883. On the characters of the skull in the Hadrosauridae. Proceedings of the Academy of Natural Sciences of Philadelphia, **35**: 97–110.

Damuth, J., and Janis, C.M. 2011. On the relationship between hypsodonty and feeding ecology in ungulate mammals, and its utility in palaeoecology. Biological Reviews, **86**: 733–758. doi:10.1111/j.1469-185X.2011.00176.x.

Dodson, P. 1975. Taxonomic implications of relative growth in lambeosaurine hadrosaurs. Systematic Zoology, **24**: 37–54.

Dodson, P., Forster, C.A., and Sampson, S.D. 2004. Ceratopsidae. *In* The Dinosauria, Second. *Edited by* D.B. Weishampel, P. Dodson, and H. Osmolska. University of California Press, Berkeley, California. pp. 494–513.

Edmund, G.A. 1960. Tooth replacment phenomena in the lower vertebrates. Life Sciences Division, Royal Ontario Museum Toronto, **52**: 3–190.

Erickson, G.M. 1996. Incremental lines of von Ebner in dinosaurs and the assessment of tooth replacement rates using growth line counts. Proceedings of the National Academy of Sciences of the United States of America, **93**: 14623–14627. doi:10.1073/pnas.93.25.14623.

Erickson, G.M., Krick, B.A., Hamilton, M., Bourne, G.R., Norell, M.A., Lilleodden, E., and Sawyer, W.G. 2012. Complex dental structure and wear biomechanics in Hadrosaurid dinosaurs. Science, **338**: 98–101. doi:10.1126/science.1224495.

Erickson, G.M., Sidebottom, M.A., Kay, D.I., Turner, K.T., Ip, N., Norell, M.A., Sawyer, W.G., and Krick, B.A. 2015. Wear biomechanics in the slicing dentition of the giant horned dinosaur *Triceratops*. Evolutionary Biology, **1**: 1–7. doi:10.11.26/sciadv.1500055.

Erickson, G.M., and Zelenitsky, D.K. 2014. Osteohistology and occlusal morphology of *Hypacrosaurus stebingeri* teeth throughout ontogeny with comments on wear-induced form and function. *In* Hadrosaurs. *Edited by* D.A. Eberth and D.C. Evans. Indiana University Press, Bloomington. pp. 422–432.

Evans, D.C. 2010. Cranial anatomy and systematics of *Hypacrosaurus altispinus*, and a comparative analysis of skull growth in lambeosaurine hadrosaurids (Dinosauria: Ornithischia). Zoological Journal of the Linnean Society, **159**: 398–434. doi:10.1111/j.1096-3642.2009.00611.x.

Evans, D.C., and Reisz, R. 2007. Anatomy and relationships of Lambeosaurus magnicristatus, a crested hadrosaurid dinosaur (Ornithischia) from the Dinosaur Park Formation, Alberta. Journal of Vertebrate Paleontology, **27**: 373–393.

Fastovsky, D.E., and Smith, J.B. 2004. Dinosaur paleoecology. *In* The Dinosauria, Second. *Edited by* D.B. Weishampel, P. Dodson, and H. Osmolska. University of California Press, Berkeley, California. pp. 614–626.

Fiorillo, A.R., and Gangloff, R.A. 2001. The caribou migration model for arctic hadrosaurs (Dinosauria: Ornithischia): a reassessment. Historical Biology, **15**: 323–334. doi:10.1080/0891296021000037327.

Fong, R.K.M., LeBlanc, A.R.H., Berman, D.S., and Reisz, R.R. 2016. Dental histology of *Coelophysis bauri* and the evolution of tooth attachment tissues in early dinosaurs. Journal of Morphology, **277**: 916–924. doi:10.1002/jmor.20545.

Fosse, G., Saele, P.K., and Eide, R. 1992. Numerical density and distributional pattern of dentin tubules. Acta Odontologica Scandinavica, **50**: 201–210. doi:10.3109/00016359209012764.

Fricke, H.C., Rogers, R.R., and Gates, T.A. 2009. Hadrosaurid migration: inferences based on stable isotope comparisons among Late Cretaceous dinosaur localities. Paleobiology, **35**: 270–288. doi:10.1666/08025.1.

Gangloff, R.A., and Fiorillo, A.R. 2010. Taphonomy and paleoecology of a bonebed from the

Prince Creek Formation, North Slope, Alaska. Palaios, **25**: 299–317. doi:10.2110/palo.2009.p09-103r.

García, R.A., and Zurriaguz, V. 2015. Histology of teeth and tooth attachment in titanosaurs (Dinosauria; Sauropoda). Cretaceous Research, **57**: 248–256. Elsevier Ltd. doi:10.1016/j.cretres.2015.09.006.

Gates, T.A. 2007. Taxonomy, biogeography, and paleoecology of North American hadrosaurid (Ornithopoda) dinosaurs. The University of Utah.

Goldberg, M., Kulkarni, A.B., Young, M., and Boskey, A. 2011. Dentin: structure, composition and mineralization: the role of dentin EMC in dentin formation and mineralization. Frontiers in bioscience (Elite edition), **3**: 711–735. doi:10.2741/e281.

Gomes, J.R., Omar, N.F., Do Carmo, E.R., Neves, J.S., Soares, M.A.M., Narvaes, E.A., and Novaes, P.D. 2013. Relationship between cell proliferation and eruption rate in the rat incisor. Anatomical Record, **296**: 1096–1101. doi:10.1002/ar.22712.

Gonçalves, P.F., Sallum, E.A., and Sallum, A.W. 2005. Dental cementum reviewed: development, structure, composition, regeneration and potential functions. Brazilian Journal Of Oral Sciences, **4**: 651–658. Available from http://www.bioline.org.br/pdf?os05003.

Gordon, L.M., Cohen, M.J., MacRenaris, K.W., Pasteris, J.D., Seda, T., and Joester, D. 2015. Amorphous intergranular phases control the properties of rodent tooth enamel. Science, **347**: 746–750.

Gowgiel, J.M. 1961. Eruption of irradiation-produced rootless teeth in monkeys. Journal of Dental Research, **40**: 538–547. doi:10.1177/00220345610400032201.

Hirschfeld, Z., Weinreb, M.M., and Michaeli, Y. 1973. Incisors of the rabbit: morphology, histology, and development. Journal of Dental Research, **52**: 377–384. doi:10.1177/00220345730520023201.

Horner, J.R., and Currie, P.J. 1994. Embryonic and neonatal morphology and ontogeny of a new species of *Hypacrosaurus* (Ornithischia, Lambeosauridae) from Montana and Alberta. *In* Dinosaur Eggs and Babies. *Edited by* K. Carpenter, K.F. Hirsch, and J.R. Horner. Cambridge University Press, Cambridge. pp. 312–336.

Horner, J.R., Weishampel, D.B., and Forster, C.A. 2004. Hadrosauridae. *In* The Dinosauria, Sedond. *Edited by* D.B. Weishampel, P. Dodson, and H. Osmolska. University of California Press, Berkeley, California. pp. 438–463.

Hwang, S.H. 2005. Phylogenetic patterns of enamel microstructure in dinosaur teeth. Journal of Morphology, **266**: 208–240. doi:10.1002/jmor.10372.

Hwang, S.H. 2011. The evolution of dinosaur tooth enamel microstructure. Biological Reviews, **86**: 183–216. doi:10.1111/j.1469-185X.2010.00142.x.

Jones, S.J., and Boyde, A. 1984. Ultrastructure of dentin and dentinogenesis Volume 1. *In* Dentin and dentinogenesis. *Edited by* A. Linde. CRC Press, Boca Raton. pp. 81–134.

von Koenigswald, W., and Mörs, T. 2001. The enamel microstructure of *Anchitheriomys* (Rodentia, Mammalia) in comparison with that of other beavers and of porcupines. Paläontologische Zeizschrift, **74**: 601–612.

Kraw, A.G., and Enlow, D.H. 1967. Continuous attachment of the periodontal membrane. American Journal of Anatomy, **120**: 133–147. doi:10.1002/aja.1001200111.

Lambe, L.M. 1920. The hadrosaur *Edmontosaurus* from the Upper Cretaceous of Alberta. Canada Department of Mines, Geological Survey of Canada Memoir, **120**: 1–79.

LeBlanc, A.R.H., and Reisz, R.R. 2013. Periodontal ligament, cementum, and alveolar bone in the oldest herbivorous tetrapods, and their evolutionary significance. PLoS ONE, **8**: 11. doi:10.1371/journal.pone.0074697.

LeBlanc, A.R.H., and Reisz, R.R. 2015. Patterns of tooth development and replacement in captorhinid reptiles: a comparative approach for understanding the origin of multiple tooth rows. Journal of Vertebrate Paleontology, **35**: e919928. doi:10.1080/02724634.2014.919928.

LeBlanc, A.R.H., Reisz, R.R., Brink, K.S., and Abdala, F. 2016a. Mineralized periodontia in extinct relatives of mammals shed light on the evolutionary history of mineral homeostasis in periodontal tissue maintenance. Journal of Clinical Periodontology, **43**: 323–332. doi:10.1111/jcpe.12508.

LeBlanc, A.R.H., Reisz, R.R., Evans, D.C., and Bailleul, A.M. 2016b. Ontogeny reveals function and evolution of the hadrosaurid dinosaur dental battery. BMC Evolutionary Biology, **16**: 152. BMC Evolutionary Biology. doi:10.1186/s12862-016-0721-1.

Listgarten, M.A. 1968. A light and electron microscopic study of coronal cementogenesis. Archives of Oral Biology, **13**: 93–114.

Lull, R.S., and Wright, N.E. 1942. Hadrosaurian dinosaurs of North America. Geological Society of America Special Papers, **40**: 1–242.

Mallon, J.C., and Anderson, J.S. 2014. The functional and palaeoecological implications of tooth morphology and wear for the megaherbivorous dinosaurs from the Dinosaur Park Formation (upper Campanian) of Alberta, Canada. Plos One, **9**: e98605. doi:10.1371/journal.pone.0098605.

Mallon, J.C., and Anderson, J.S. 2015. Jaw mechanics and evolutionary paleoecology of the megaherbivorous dinosaurs from the Dinosaur Park Formation (upper Campanian) of Alberta, Canada. Journal of Vertebrate Paleontology Publication, **35**: e904323. doi:10.1080/02724634.2014.904323.

Martin, T. 1994. On the systematic position of *Chaetomys subspinosus* (Rodentia: Caviomorpha) based on evidence from the incisor enamel microstructure. Journal of Mammalian

Evolution, **2**: 117–131.

Martin, T. 2004. Evolution of incisor enamel microstructure in Lagomorpha. Journal of Vertebrate Paleontology, **24**: 411–426.

Maxwell, E.E., Caldwell, M.W., and Lamoureux, D.O. 2011a. Tooth histology in the cretaceous ichthyosaur *Platypterygius australis*, and its significance for the conservation and divergence of mineralized tooth tissues in amniotes. Journal of Morphology, **272**: 129–135. doi:10.1002/jmor.10898.

Maxwell, E.E., Caldwell, M.W., Lamoureux, D.O., and Budney, L.A. 2011b. Histology of tooth attachment tissues and plicidentine in *Varanus* (Reptilia: Squamata), and a discussion of the evolution of amniote tooth attachment. Journal of Morphology, **272**: 1170–1181. doi:10.1002/jmor.10972.

Michaeli, Y., Zajicek, G., and Ginio, I. 1977. Cell production in the normal and lathyrogenic rat periodontal ligament (PDL). Journal of Dental Research, **58**: 511–515.

Mjör, I.A., and Nordahl, I. 1996. The density and branching of dentinal tubules in human teeth. Archives of Oral Biology, **41**: 401–412.

Møinichen, C.B., Lyngstadaas, S.P., and Risnes, S. 1996. Morphological characteristics of mouse incisor enamel. Journal of anatomy, **189**: 325–33.

Morris, W.J. 1970. Hadrosaurian dinosaur bills -morphology and function. Contributions in Science,: 1–14.

Nabavizadeh, A. 2014. Hadrosauroid jaw mechanics and the functional significance of the predentary bone. *In* Hadrosaurs. *Edited by* D.A. Eberth and D.C. Evans. Indiana University Press, Bloomington. pp. 467–482.

Nanci, A. 2013. Ten Cate's oral histology: development, structure and function. *In* 8th Editio. Elsevier, Amsterdam.

Ohshima, H., and Yoshida, S. 1992. The relationship between odontoblasts and pulp capillaries in the process of enamel- and cementum-related dentin formation in rat incisors. Cell & Tissue Research, **268**: 51–63. doi:10.1007/BF00338053.

Osborn, J.W. 1969. Dentine hardness and incisor wear in the beaver (*Castor fiber*). Acta Anatomica, **72**: 123–132.

Ostrom, J.H. 1961. Cranial morphology of the hadrosaurian dinosaurs of North America. Bulletin of the American Museum of Natural History, **122**.

Parks, W.A. 1922. *Parasaurolophus walkeri*, a new genus and species of crested trachodont dinosaur. University of Toronto Studies: Geological Series, **13**: 5–32.

Pretto, F.A., Cabreira, S.F., and Schultz, C.L. 2014. Tooth microstructure of the Early Permian aquatic predator *Stereosternum tumidum*. Acta Palaeontologica Polonica, **59**: 125–133. doi:10.4202/app.2011.0121.

Prieto-Márquez, A. 2008. Phylogeny and historical biogeography of hadrosaurid dinosaurs. Florida State University Thesis,: 861.

Reid, R.E.H. 1996. Bone histology of the Cleveland-Lloyd dinosaurs and of dinosaurs in general, part I: introduction: introduction to bone tissues. Brigham Young University Geology Studies, **41**: 25–72.

Rinaldi, C., and Cole, T.M. 2004. Environmental seasonality and incremental growth rates of beaver (*Castor canadensis*) incisors: implications for palaeobiology. Palaeogeography, Palaeoclimatology, Palaeoecology, **206**: 289–301. doi:10.1016/j.palaeo.2004.01.008.

Rosenberg, G.D., and Simmons, D.J. 1980. Rhythmic Dentinogenesis in the rabbit Incisor: allometric aspects. Calcified Tissue International, **32**: 45–53.

Saffar, J.L., Lasfargues, J.J., and Cherruau, M. 1997. Alveolar bone and the alveolar process: the socket that is never stable. Periodontology 2000, **13**: 76–90. doi:10.1111/j.1600-

0757.1997.tb00096.x.

Sander, P.M. 1997. Teeth and Jaws. *In* Encyclopedia of Dinosaurs. *Edited by* P.J. Currie and K. Padian. Academic Press, San Diego. pp. 717–725.

Sander, P.M. 1999. The microstructure of reptilian tooth enamel: terminology, function, and phylogeny. Münchner Geowissenschaftliche Abhandlungen, **38**: 1–102. Münchner Geowissenschaftliche Abhandlungen Reihe A.

Schneider, C.A., Rasband, W.S., and Eliceiri, K.W. 2012. NIH Image to ImageJ: 25 years of image analysis. Nature Methods, **9**: 671–675. Nature Publishing Group. doi:10.1038/nmeth.2089.

Schour, I., and Steadman, S.R. 1935. The growth pattern and daily rhythm of the incisor of the rat. The Anatomical Record, **63**: 325–333.

Schwarz, D., Kosch, J.C.D., Fritsch, G., and Hildebrandt, T. 2015. Dentition and tooth replacement of *Dicraeosaurus hansemanni* (Dinosauria, Sauropoda, Diplodocoidea) from the Tendaguru Formation of Tanzania. Journal of Vertebrate Paleontology, **35**: e1008134. doi:10.1080/02724634.2015.1008134.

Shellis, P. 1981. Dentine. *In* Dental anatomy and embryology. *Edited by* J.W. Osborn. Blackwell Scientific Publications, Oxford. pp. 166–174.

Shellis, P., and Berkovitz, B.K.B. 1981. The dentition of laboratory rodents and lagomorphs. *In* Dental anatomy and embryology. *Edited by* J.W. Osborn. Blackwell Scientific Publications, Oxford. pp. 432–439.

Smith, J.B., and Dodson, P. 2003. A proposal for a standard terminology of anatomical notation and orientation in fossil vertebrate dentitions. Journal of Vertebrate Paleontology, **23**: 1–12. The Society of Vertebrate Paleontology.

Stefen, C., Habersetzer, J., and Witzel, U. 2016. Biomechanical aspects of incisor action of beavers (*Castor fiber* L.). Journal of Mammalogy, **97**: 619–630.

Stein, G., and Boyle, P.E. 1959. Pigmentation of the enamel of albino rat incisor teeth. Archives of Oral Biology, **1**: 97–105.

Steinfort, J., Deblauwe, B.M., and Beertsen, W. 1990. The inorganic components of cementum- and enamel-related dentin in the rat incisor. Journal of Dental Research, **69**: 1287–1292. doi:10.1177/00220345900690061301.

Tweet, J.S., Chin, K., Braman, D.R., and Murphy, N.L. 2008. Probable gut contents within a specimen of *Brachylophosaurus canadensis* (Dinosauria: Hadrosauridae) from the Upper Cretaceous Judith River Formation of Montana. Palaios, **23**: 624–635. doi:10.2110/palo.2007.p07-044r.

Vanderven, E., Burns, M.E., Currie, P.J., and Farke, A. 2014. Histologic growth dynamic study of *Edmontosaurus regalis*(Dinosauria: Hadrosauridae) from a bonebed assemblage of the Upper Cretaceous Horseshoe Canyon Formation, Edmonton, Alberta, Canada 1. Canadian Journal of Earth Sciences, **51**: 1023–1033. doi:10.1139/cjes-2014-0064.

Vignery, A., and Baron, R. 1980. Dynamic histomorphometry of alveolar bone remodeling in the adult rat. Anatomical Record, **196**: 191–200.

Wang, C.C., Song, Y.F., Song, S.R., Ji, Q., Chiang, C.C., Meng, Q.J., Li, H.B., Hsiao, K., Lu, Y.C., Shew, B.Y., Huang, T., and Reisz, R.R. 2015. Evolution and function of dinosaur teeth at ultramicrostructural level revealed using synchrotron transmission x-ray microscopy. Scientific Reports, **5**: 11. Nature Publishing Group. doi:10.1038/srep15202.

Weishampel, D.B. 1983. Hadrosaurid jaw mechanics. Acta Palaeontologica Polonica, **28**: 271–280.

Williams, V.S., Barrett, P.M., and Purnell, M. a. 2009. Quantitative analysis of dental microwear in hadrosaurid dinosaurs, and the implications for hypotheses of jaw mechanics and feeding.

Proceedings of the National Academy of Sciences of the United States of America, **106**: 11194–11199. doi:10.1073/pnas.0812631106.

Witmer, L.M. 1995. The extant phylogenetic bracket and the importance of reconstructing soft tissues in fossils. *In* Functional morphology in vertebrate paleontology. *Edited by* J.J. Thomason. Cambridge University Press, New York. pp. 19–33.

Woodward, H.N., Freedman Fowler, E.A., Farlow, J.O., and Horner, J.R. 2015. *Maiasaura*, a model organism for extinct vertebrate population biology: a large sample statistical assessment of growth dynamics and survivorship. Paleobiology, **41**: 503–527. doi:10.1017/pab.2015.19.

Xing, H., Wang, D., Han, F., Sullivan, C., Qingyu, M., He, Y., Hone, D.W.E., Yan, R., Du, F., and Xu, X. 2014. A new basal hadrosauroid dinosaur (Dinosauria: Ornithopoda) with transitional features from the Late Cretaceous of Henan Province, China. PLoS ONE, **9**: 7–10. doi:10.1371/journal.pone.0098821.